

Review

# A Review on MoS<sub>2</sub> Properties, Synthesis, Sensing Applications and Challenges

Omnia Samy <sup>1</sup>, Shuwen Zeng <sup>2</sup>, Muhammad Danang Birowosuto <sup>3,4</sup> and Amine El Moutaouakil <sup>1,\*</sup>

<sup>1</sup> College of Engineering, United Arab University, P.O. Box 15551, Al Ain 15551, United Arab Emirates; 202090009@uaeu.ac.ae

<sup>2</sup> XLIM Research Institute, UMR 7252 CNRS/University of Limoges, 123, Avenue Albert Thomas, 87060 Limoges CEDEX, France; zeng@xlim.fr

<sup>3</sup> CNRS International-Nanyang Technological University (NTU), Thales Research Alliance (CINTRA), Singapore 637553, Singapore; mbirowosuto@ntu.edu.sg

<sup>4</sup> Department of Renewable Energy Engineering, Universitas Prasetiya Mulya, Kavling Edutown I.1, Jl. BSD Raya Utama, BSD City, Tangerang 15339, Indonesia

\* Correspondence: a.elmoutaouakil@uaeu.ac.ae

**Abstract:** Molybdenum disulfide (MoS<sub>2</sub>) is one of the compounds discussed nowadays due to its outstanding properties that allowed its usage in different applications. Its band gap and its distinctive structure make it a promising material to substitute graphene and other semiconductor devices. It has different applications in electronics especially sensors like optical sensors, biosensors, electrochemical biosensors that play an important role in the detection of various diseases' like cancer and Alzheimer. It has a wide range of energy applications in batteries, solar cells, microwave, and Terahertz applications. It is a promising material on a nanoscale level, with favorable characteristics in spintronics and magnetoresistance. In this review, we will discuss MoS<sub>2</sub> properties, structure and synthesis techniques with a focus on its applications and future challenges.



**Citation:** Samy, O.; Zeng, S.; Birowosuto, M.D.; El Moutaouakil, A. A Review on MoS<sub>2</sub> Properties, Synthesis, Sensing Applications and Challenges. *Crystals* **2021**, *11*, 355. <https://doi.org/10.3390/cryst11040355>

Academic Editor: Dmitri Donetski

Received: 24 February 2021

Accepted: 23 March 2021

Published: 29 March 2021

**Publisher's Note:** MDPI stays neutral with regard to jurisdictional claims in published maps and institutional affiliations.



**Copyright:** © 2021 by the authors. Licensee MDPI, Basel, Switzerland. This article is an open access article distributed under the terms and conditions of the Creative Commons Attribution (CC BY) license (<https://creativecommons.org/licenses/by/4.0/>).

## 1. Introduction

Molybdenum disulfide (MoS<sub>2</sub>) is an inorganic compound of the transition metal dichalcogenides (TMDs) series, that has one atom of Molybdenum and two atoms of Sulfur. Dichalcogenides are chemical compounds consisting of a transition metal, like Molybdenum, and a chalcogen (element of group 16 in the periodic table) like sulfur (S) [1]. The physical, chemical, and electronic properties of this compound grabbed the attention of many researchers and were found promising materials to substitute previously used semiconductor and/or graphene devices. As the world is moving towards miniaturization, researchers were searching for a material to substitute semiconductor devices that seemed to reach an end when entering the nanoscale era [2]. While semiconductors devices based on Silicon were facing quantum and tunneling effects on a nanoscale level, MoS<sub>2</sub> showed favorable and promising electronic and quantum characteristics when going from bulk to two-dimensional (2D) structure [3].

MoS<sub>2</sub> seems to solve many problems facing previous devices [4–8], it has a large band gap (~1.8 eV) which changes from an indirect gap to a direct one in thin structures. This would permit downscaling electronic devices, rather than graphene which nearly has a zero-band gap [9,10]. It does not have surface dangling bonds and has high mobility even with high- $\kappa$  dielectric materials. It is ideal for thin-film transistors, and its fabrication is simple which means large production yield and low cost [11,12]. The covalent bonds between Molybdenum and Sulfur and the Van der Waals bonds between its layers make it optimal for gas sensing. One of the major problems with Silicon devices was that related

to the metal-semiconductor interface [13]. MoS<sub>2</sub> has less contact resistance and high performance. In other words, MoS<sub>2</sub> has potency to be used in 1 nm gate transistors with excellent on/off switching characteristics and high efficiency [14].

Silicon transistors fabrication faced some problems on the bulk scale that were overcome by new structures such as multi-gate transistors, but when going down to the nanoscale, the fabrication process seems to reach an end. The metal interconnection lines between transistors have high density and are very narrow, which cause an increase in resistance and capacitance between interconnect lines and high delays. Tunneling problems are more obvious with thin gate oxides and when trying to substitute silicon dioxide with other high- $\kappa$  dielectric materials, more serious problems like thermal instability, channel mobility degradation, incompatibility with the interface aroused. All these issues lead to performance degradation, and high cost with a small yield. The high lithography resolution needed for small half-pitch (HP) ~20 nm, is not easily achieved and needs high techniques and tools in lithography [15,16]. On the other side, MoS<sub>2</sub> showed easier and simpler ways of synthesis and device fabrication [17]. It is easily prepared by spreading the molybdenum metal and sulfur and letting them self-propagate under a high temperature [18]. A MoS<sub>2</sub> field effect transistor was fabricated in [19] by immersing it in an electrolyte, the device showed lower contact resistance and a better gate control.

MoS<sub>2</sub> has a wide range of applications in different fields. Like Silicon and graphene, it has applications in biosensing, and optical sensors but the most important ones are those related to bio-applications like DNA, cancer, and Corona Virus detection [20–23]. While Silicon and graphene were still under study in their compatibility with human bodies, a study, in [24], showed that MoS<sub>2</sub> may be very effective in curing cancer and Alzheimer's disease. It also showed that the compound has no biological interaction which makes it safe for injection in human bodies. Another study in [25] proposed a biocompatible device made of MoS<sub>2</sub> to restore some visual malfunctioning. The compound applications are not restricted to electronics, but it can serve as a lubricant [26] and is used in hydrogen evolution reactions. It is a suitable material for batteries' electrodes [27]. Indeed, MoS<sub>2</sub> properties and structure made it promising for several electronic, sensing, microwave, and terahertz applications.

Many research articles and reviews have been published on the properties, synthesis and applications of MoS<sub>2</sub> material, but we lack a comprehensive comparison of the different MoS<sub>2</sub> structures and their properties in terms of applications, especially between the bulk and monolayer MoS<sub>2</sub>. Besides, the use of MoS<sub>2</sub> as a sensing material in the bio-medical, optoelectronic and IoT-related fields was not sufficiently highlighted in the literature. Newer applications such as in the terahertz technology, the hydrogen detection, hydrogen generation and oil/water separation remain among the less covered areas of studies for MoS<sub>2</sub>. In this review, we will first identify the different MoS<sub>2</sub> structures and their synthesizing techniques in details, and we will compare all the structures in terms of their main optical, lattice and electrical properties and applications. Synthesis techniques will be extensively covered with their main pros and cons. Then we will provide a more detailed review on the wide range applications of MoS<sub>2</sub> in electronics, medicine and other new fields of research such as the terahertz field and the hydrogen-related technologies. Finally, we will discuss and compare the different challenges facing the development of MoS<sub>2</sub> applications in different fields of study, since they were not discussed in detail in previous studies that focused more on synthesizing techniques [27,28] or a specific kind of application [29–31].

## 2. Structure and Properties

MoS<sub>2</sub> structures differ from 3D, 2D, one-dimensional (1D), or dot structures. Its characteristics and applications also change from one dimension to another, they can be semiconducting, metallic or superconducting. It exists in several layers and shapes. Its bulk (3D) structure can be tri-agonal (T), hexagonal (H), and Rhombohedral (R), where 2H MoS<sub>2</sub> means 2-layer hexagonal shape MoS<sub>2</sub>. The three main structures are 1T, 2H and

3R, where the 1T phase coordinates in an octahedral structure, 2H and 3R in a trigonal prismatic structure [32,33] as shown in Figure 1. The lattice constants for each structure are shown in Table 1 [34]. The 1T structure is known to be metallic while the other two are semiconducting. The monolayer of hexagonal MoS<sub>2</sub> is also semiconducting. Both 2H and 3R are used as dry lubricants. Due to the nonlinear optical mass sensing in quantum measurements and biomedicine [35]. As an example, for gas sensors, the different phase materials of MoS<sub>2</sub> can be interesting in obtaining high sensitivity and rapid desorption [36].

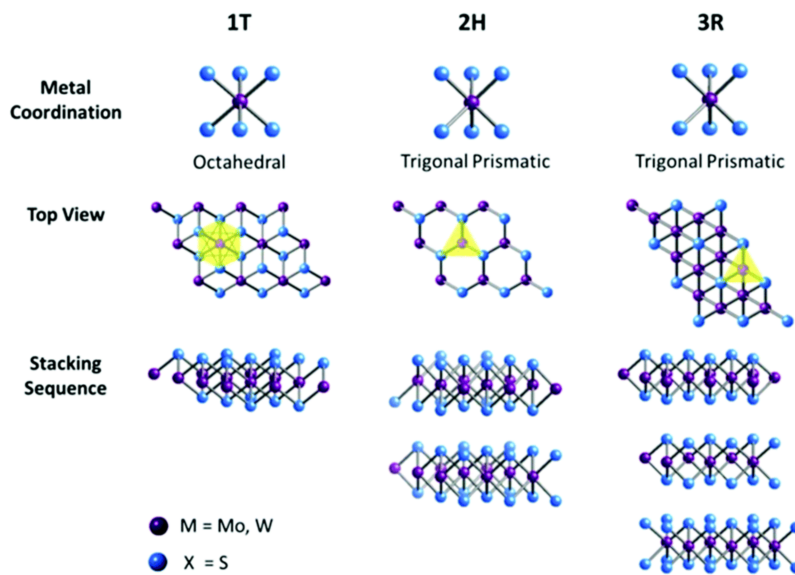


**Figure 1.** Different coordination and stacking sequences of the three MoS<sub>2</sub> structures 1T, 2H and 3R. Reproduced from [33]. Published by The Royal Society of Chemistry.

**Table 1.** Comparison between different MoS<sub>2</sub> structures.

	1T	2H	3R
Structure Coordination	Octahedral	Trigonal Prismatic	Trigonal Prismatic
Lattice parameters	$a = 5.60 \text{ \AA}$ , $c = 5.99 \text{ \AA}$ and an edge sharing octahedral [34]	$a = 3.15 \text{ \AA}$ , $c = 12.30 \text{ \AA}$ [34]	$a = 3.17 \text{ \AA}$ , $c = 18.38 \text{ \AA}$ [34]
property	paramagnetic and metallic		Semiconducting
Electrical conductivity	$10^5$ times higher than 2H phase	Low ( $\sim 0.1 \text{ S/m}$ )	
Absorption peaks	No peaks at 604 nm and 667 nm	Showed peaks at 604 nm and 667 nm	
Common applications	Intercalation in chemistry	Dry lubricants	Dry lubricants and non-linear optical devices

1H MoS<sub>2</sub> is the most stable configuration and it is formed of one layer of Sulfur and one layer of Mo where S-Mo-S are attached through strong covalent bond like a sandwich, with a thickness of approximately 0.65 nm [28]. The sandwiched S-Mo-S layers are attached through weak Wannier Val forces [37]. The conductivity of nano MoS<sub>2</sub> depends on the temperature and thickness of the flakes, where conductivity increases with the temperature increase and decreases with increasing the thickness till it reaches the bulk structure [38]. The binding energies and photoluminescence properties are summarized in Table 2 [39].

**Table 2.** Comparison between Bulk and monolayer MoS<sub>2</sub>.

	Bulk	Monolayer
Bandgap	Indirect (~1.2 eV)	Direct (1.8 eV)
Binding energy	0.1 eV	1.1 eV
Photoluminescence intensities	between $10^{-5}$ and $10^{-6}$	$10^4$ times higher than that of bulk, up to and up to $4 \times 10^{-3}$

MoS<sub>2</sub> exists in different 2D structure like nanosheets, and nanoribbons or 1D structures as nanowires and nanotubes, or 0D structure as quantum dots and nanoplatelets. The thickness of 2D nanoribbons was found to be of 1 to 3 layers of MoS<sub>2</sub>, while the thickness of 1D nanowires (NW) can have lengths from 14 to 30 nm and a width of 0.6 nm approximately [40]. The structure of 1D nanoplatelets and their properties were investigated in [41]. The nanoplatelets are 12–30 nm with one-unit cell width. They have very high catalytic activity for hydrodesulphurization. The quantum dots range from 2 to 10 nm in size. They have higher band gap than nanosheets, and stronger bonds between Mo atoms than monolayers. The change in band gap of MoS<sub>2</sub> from one dimension to another, changes the photoluminescence characteristics and thus has different optical properties according to its dimension. Additionally, monolayers or other low dimension forms are also easy to be implemented in optical nanostructures to enhance the photoluminescence intensities and emission rates through light-matter interactions [42–44]. This is a strong motivation for MoS<sub>2</sub> to be included in optical applications [29].

### 2.1. Optical Properties

The absorption coefficient and refractive index are the parameters that determine the response of a material when a certain wavelength passes through it. The absorption coefficient determines the distance the spectrum pass inside the material before being absorbed. A high absorption coefficient means high attenuation to the wave applied. Semiconductors have high absorption coefficients for short wavelengths (high energy and frequency spectrum) and low absorption coefficients for long wavelengths (they do not have enough energy to excite electrons from the valence band to the conduction band). MoS<sub>2</sub> has a relatively large absorption coefficient for the wavelengths from 400 nm to 500 nm with a sharp decay at 500 nm [45]. The key factor behind the wide use of MoS<sub>2</sub> in optoelectronics is its tunable bandgap that changes with size and structure; Different bandgaps mean tunable photoresponsivity (R), specific detectivity, and response time [46], and thus, a wide range of applications. The MoS<sub>2</sub> multilayers and monolayers have a high refractive index of more than 2, where it can be used in coating. Since the photoluminescence (PL) spectra are affected by the band gap, doping, and structure of the material, MoS<sub>2</sub> has different PL activity. It has a peak exciton (A) in a single layer MoS<sub>2</sub>. The PL properties of monolayer MoS<sub>2</sub> are enhanced by adding H<sub>2</sub>O<sub>2</sub> solution [47], where it acts as a strong oxidizer without changing the crystalline structure of MoS<sub>2</sub>. TMDs are known for their low PL quantum yield (QY) which is the ratio of the number of emitted photons to the number of generated electron-hole pairs and they are between 0.01 to 6%. The work in [48] was able to raise the QY of MoS<sub>2</sub> to 95% using a chemical treatment of an organic superacid. The observed lifetime of MoS<sub>2</sub> carriers were nearly 10.8 ns, which opens the way to be used in high-performance lasers and solar cells.

### 2.2. Mechanical Properties

A monolayer MoS<sub>2</sub> has high strength, less than that of graphene and good elasticity similar to that of graphene oxide, with Young's modulus of  $0.33 \pm 0.07$  TPa [28]. A single layer of MoS<sub>2</sub> has more flexibility than bulk structures, where its Young's modulus is 0.24 TPa. Unlike other semiconductors, the flexibility of MoS<sub>2</sub> prevents the deformation and band gap shifts that may happen to its crystalline structure when subjected to strain. However, the mechanical strain is used to alter MoS<sub>2</sub> electronic characteristics and trans-

form them from semiconductors to metals. It transforms the direct band gap of MoS<sub>2</sub> monolayers to an indirect one and high strain values can cause structure deformation and transform MoS<sub>2</sub> to metal [49].

### 2.3. Electronic Properties

In this section, we are going to discuss the density of states and the band structure of MoS<sub>2</sub>. Multilayer MoS<sub>2</sub> are known to have an indirect band gap of 1.2 eV, which increase with the decrease in the number of layers until we have a direct band gap of 1.8 eV in monolayer MoS<sub>2</sub> [50]. Although the MoS<sub>2</sub> bandgap value is good, it is still far from 1.12 eV direct bandgap of Silicon [39]. The mechanical strain affects the band gap of MoS<sub>2</sub> and changes it from direct to indirect band gap and transfers the material from a semiconducting material to a metallic one. The 4d and 3p orbitals in Mo and S respectively, determines the properties of MoS<sub>2</sub>. The projected density of states (PDOS) of bulk and monolayer MoS<sub>2</sub> are nearly the same, but there are some peaks in PDOS in case of monolayer MoS<sub>2</sub> [51]. A monolayer MoS<sub>2</sub> changes to an n-type semiconductor when doped with chromium, copper, and scandium (Sc) and to a p-type when doped with Nickel or Zinc [52]. Doping with Titanium (Ti) transfers MoS<sub>2</sub> to a p-type or n-type semiconductor according to the levels and sites of doping. At low doping levels of Ti below 2.04%, MoS<sub>2</sub> behaves as a p-type. In case of interstitial doping of Titanium (Ti) at 3.57% doping levels, the covalent bond between MoS<sub>2</sub> and Ti are strong which increases the surface dipole moment that induces a reduction in electron affinity of 0.49 eV, where it behaves as an n-type. At high doping levels of 7.69%, the Fermi level shifts towards the conduction band and merge into the conduction band, where the surface dipole moment declines and the electron affinity rises, pinning Fermi level over the conduction band. In this case, MoS<sub>2</sub> changes to a ferromagnetic half-metal with spin polarization equals to 1, that is promising for spintronics. On the other side the substitutional doping of Ti did not show any change in electronic properties for the three doping concentrations (2.04%, 3.57%, 7.69%).

### 2.4. Magnetic Properties (Spintronics)

While moving towards the nanoscale era and the evolution of spintronics, the study of electron spin of a promising structure like MoS<sub>2</sub> became a must. TMDs are known to be non-magnetic, and if we managed to add magnetism to them, they can be used as tunable semiconductors [53]. A study in [54] studied the magnetic behavior and characteristics of multilayer MoS<sub>2</sub> specifically. The study showed that MoS<sub>2</sub> has a long spin diffusion length of 235 nm and that an in-plane spin polarization can suppress the electron spin-relaxation. The work in [52] showed that MoS<sub>2</sub> attains semi-metallic ferromagnetic properties when doped with Sc and a unity spin polarization value, which is favorable in spintronics.

## 3. Synthesis

There are different techniques used to obtain material layers Figure 2, and each one of them results in different quantities, shapes, and sizes. Mainly the approaches used in synthesizing TMDs nanostructures, are the top-down approach and the bottom-up approach [55,56]. The first approach depends on etching crystal planes from a substrate that has the crystals laid over it, while in the second approach, the crystals are stacked over the substrate. Exfoliation is one of the top-bottom techniques for obtaining MoS<sub>2</sub> layers. The weak Van der Waal forces between layers of TMDs paved the way in front of different exfoliation synthesizing techniques [57]. Mechanical exfoliation is done using a sticky tape which is rubbed out and shifted on a substrate having MoS<sub>2</sub> flakes over it. The method gives low yield and is good for lab use. Exfoliation can also be done in the liquid phase by adding a chemical compound and stirring, bubbling, or grinding. This method is simple and cheap but has low quality. The low yield in liquid exfoliation was avoided using carbon aerogel composites in [58]. The synthesizing is fast and completed in 30 minutes. It also avoids pyrophoric materials that are typically used in liquid exfoliation and increases the electrical conductivity and porosity of MoS<sub>2</sub>. Sonication is one of the techniques that

showed simple synthesis when used with liquid exfoliation [59,60]. It dispenses of the use of hazardous materials used in liquid exfoliation. It is based on ultrasonic waves emitted from a probe in shape of bubbles that peels MoS<sub>2</sub> layers when they burst. The challenge in using sonication assisted techniques is that it produces relatively small area MoS<sub>2</sub> nanosheets that limits its use in practical applications. Generally Top down techniques are said to have low controllability, and scalability and high cost [55]. The yield is increased to >90% when using ultrasound sonication with supercritical carbon in [61] with an intercalating solvent N-methyl-2-pyrrolidone (NMP). The method is fast, simple and scalable. Sputtering is used to prepare layers of MoS<sub>2</sub> to be used as lubricants, the layers have a low friction coefficient, but these frictional properties can be changed under humidity, especially for thin films of MoS<sub>2</sub>.

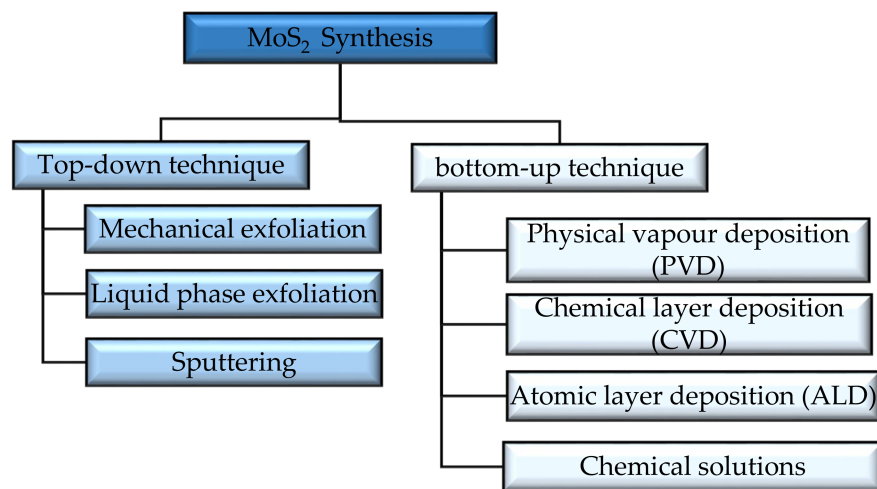


**Figure 2.** Different MoS<sub>2</sub> synthesis techniques [27].

Physical layer deposition (PVD) is one of the bottom-up techniques that includes ion implantation like molecular beam epitaxy (MBE) [62]. The method can be applied only to thin layers of MoS<sub>2</sub> and the resulting grain sizes are variable [63]. Chemical vapor deposition (CVD) is applied to thin and thick layers, where Mo is laid over a substrate and Sulfur vapor passes over it. This method has good quality, but low yield. The atomic layer deposition (ALD) method is used to fabricate thick and thin films. The method is considered efficient and the layers have fewer impurities that can be used in different applications, including electronics and sensors. MoS<sub>2</sub> layers can be synthesized with the help of chemical solutions, using hydrothermal and solvothermal reactions wherein both cases Mo and S react in an aqueous solution above the boiling point and in a nonaqueous solution at high temperature, respectively. The size and shape of the layers can be controlled where we can get powder and thin films of MoS<sub>2</sub> by this method. It is considered cheap and scalable [64].

In [65], MoS<sub>2</sub> is synthesized using a liquid organic precursor on an insulating substrate using CVD. The used method is more reproducible and is used to obtain larger areas of MoS<sub>2</sub> layers than those obtained with methods using powder Molybdenum oxide and sulfur powder. Another method in [66] used thermal evaporation and ALD, where it used metalloporphyrin as a promoter layer. The method allowed to manipulate the carrier density and conductivity of MoS<sub>2</sub> according to the thickness of the metalloporphyrin layer used. It is used to produce MoS<sub>2</sub> nanosheets on a large scale. In [18], MoS<sub>2</sub> is synthesized using self-propagating, under high temperature, where Mo nanopowders and elementary Sulfur are used. The mixture is put into cylinders and then under pressure. The main resulting structure is 2H MoS<sub>2</sub>, but there are other phases like rhombohedral MoS<sub>2</sub> and Mo<sub>2</sub>S<sub>3</sub>. Thermal sulfidation is another method like CVD that uses Sulfur gas as a precursor. It uses a Mo [67] or Mo-oxide [68] film deposited on a substrate, where evaporated sulfur passes over it under certain temperature. The method is known to reduce the effect of gas

flows that occurs in CVD, and results in self-aligned patterns of MoS<sub>2</sub>. The sulfidation of two different oxides of Mo: MoO<sub>3</sub>, and MoO<sub>2</sub> discussed in [68], showed more stable MoS<sub>2</sub> monolayer films, produced from MoO<sub>2</sub>. The films were integrated with bottom-gate transistors and they showed on/off ratio of 10<sup>3</sup>–10<sup>4</sup> and electron mobility of 10<sup>-4</sup> cm<sup>2</sup>/V·s. The PL spectrum of the synthesized monolayers has an exciton peak at 1.89 eV.

Another approach to avoid the drawbacks of exfoliation and intercalation or liquid exfoliation like low electrical performance (low mobility of 0.3–0.4 square centimeters per volt per second and low on/off ratios ~10–100) is using electrochemical intercalation [69]. The method involves quaternary ammonium molecules into 2D crystals, with mild sonication and exfoliation techniques. The technique gives high performance MoS<sub>2</sub> nanosheets with 10 square centimeters per volt per second mobility, and on/off ratios of 10<sup>6</sup>. Table 3 summarizes some synthesis techniques that are already known until now.

**Table 3.** Summary of synthesis techniques.

Technique	Characteristics of the Obtained MoS <sub>2</sub> Sheets	Publisher	Year	Reference
Using aerogel	A rapid synthesis technique for TMDs- carbon aerogel composites to be used in supercapacitor. The preparation time is 30 min which is approximately 2% of typical aerogel techniques that take 24 h	Nature	2017	[58]
Liquid assisted Sonication	Studied the PL, Raman analysis resulting from bath and probe sonication synthesis	Elsevier	2020	[59]
Liquid exfoliation & ultrasonic cavitation	Obtain less defective and high concentration nanosheets in a short time	Nature	2014	[60]
Exfoliation of & Ultrasound Sonication in Supercritical Co <sub>2</sub>	Exfoliation efficiency > 90%	Springer	2019	[61]
Exfoliation & sonication	Mobility = 10 cm <sup>2</sup> /V, on/off ratios = 10 <sup>6</sup>	Nature	2018	[69]
ALD & thermal evaporation	Enhanced electrical conductivity	Nature	2016	[66]
CVD & liquid precursor	The method uses water to remove impurities like carbon and sulphur. It ensures full coverage of MoS <sub>2</sub> for the substrate	Nature	2017	[65]
ALD & thermal evaporation	The carrier density and conductivity of MoS <sub>2</sub> are adjusted according to the thickness of the metalloporphyrin layer used. Produce large scale MoS <sub>2</sub> nanosheets	Nature	2016	[66]
Self propagation of Mo powder and elementary Sulfur	Resulted MoS <sub>2</sub> nanosheets have thermal stability up to 400 °C.	IEEE	2013	[18]
CVD with Sulfur as a precursor (Sulfidation)	on/off current ratio of 10 <sup>5</sup> , a mobility of 0.12 cm <sup>2</sup> /V·s (mean mobility value of 0.07 cm <sup>2</sup> /V·s	Royal society of chemistry	2014	[67]
Sulfidation	The on/off ratio of 10 <sup>3</sup> –10 <sup>4</sup> and electron mobility of 10 <sup>-4</sup> cm <sup>2</sup> /V·s	Elsevier	2020	[68]
Intercalation & exfoliation	To be used in high-performance thin-film transistors, on/off ratio of 10 <sup>6</sup> and electron mobility of 10 cm <sup>2</sup> /V·s	Springer Nature	2018	[69]

#### 4. Applications

MoS<sub>2</sub> optical, electrical, and chemical properties allowed this metal dichalcogenide to have a wide range of applications in different fields. Its electronic properties allowed

it to enter the nanoelectronics and sensor application field and in turn the medical field. These special electronic properties, together with its biocompatibility, open up the way to further medical and curing applications. The photoluminescence and chemical properties broadened its application field. MoS<sub>2</sub> applications are countless, and, in this review, we are trying to introduce the newest and the most important ones.

#### 4.1. Electronics Applications

In this part, we will discuss electronic, optoelectronic, and sensing applications. MoS<sub>2</sub> monolayers achieved good device characteristics at 5 nm channel length FET [70]. It has on/off ratio of 10<sup>6</sup> and a subthreshold swing of ~65 mV/decade, but with low on current of ~700 μA/μm. In [71], a 2D MoS<sub>2</sub> field effect transistor (FET) was developed to be used in operational amplifiers (OPA) in analogue circuits, the device has good performance with an open-loop gain of 36 dB at low frequency and high uniformity. The idea that MoS<sub>2</sub> can be integrated with flexible substrate materials like Kapton opens the way to be used in analogue circuits more than other bulk semiconductors. The device has acceptable bandwidth and gain (the gain roll-off after 5 kHz), compared to other Silicon devices. A heterostructure of MoS<sub>2</sub> and amorphous Silicon was developed to be used as a photodetector in [72]. The proposed photodetector has a fast response and simple fabrication so it is ideal to be used in bioimaging like x-ray imaging devices. In [73], a high-quality photodetector, including MoS<sub>2</sub> is proposed using CVD and PVD techniques. The photodetector is suitable for UV applications. It has high photocurrent gain of 1.6 and a specified detectivity of 4.32 × 10<sup>8</sup> Jones. It has external quantum efficiency (EQE), which is the amount of extracted free charge carriers converting to photo flux- of ~1.0 × 10<sup>10</sup> at 365 nm. According to the thickness of the MoS<sub>2</sub> layer used, the PL and Ramen spectra peaks are shifted. MoS<sub>2</sub> has a role in photodetectors in the field of robotics, where an efficient nanoscale photodetector of a monolayer MoS<sub>2</sub> was proposed in [74]. The detector consumes a low amount of energy (from 1 to 1000 nanojoules) with a small fingerprint of (~1 μm × 5 μm).

A Sulfur treatment with Alcohol is performed to enhance the contact resistance of MoS<sub>2</sub> FETs of gate lengths (500 to 80 nm) to be 1.3 kΩ [75]. An enhancement in the on/off switching characteristics and subthreshold swing (SS) of MoS<sub>2</sub> FET using Ag is presented in [76], where the device has SS ~4.5 mm/decade with less leakage and steep on/off characteristics. MoS<sub>2</sub> monolayer is used in nonvolatile memory applications [77], with high charge storage capacity.

A low power MoS<sub>2</sub> RF thin film transistor (TFT) was proposed in [78] that can be used in IoT systems like amplifiers and mixers. It can work at relatively high strain ~3%. The on/off ratio MoS<sub>2</sub> FETs exceeds 10<sup>8</sup> [79]. The band gap structure of TMDs can be engineered using strain, or dielectric screening [80]. Another low power analogue memory in [81] can be integrated with computing devices to enhance their efficiency. Finding a low contact resistance in TMDs based devices is still a challenge, due to the Fermi level pinning that occurs in metal/2D TMD interface, but in [82] a MoS<sub>2</sub>/MoO<sub>3</sub> tunnel field effect (TFET) was introduced, making use of oxygen vacancies in the metal oxide that aligns with the valance band of MoS<sub>2</sub> and assure a good contact with MoS<sub>2</sub>. Nanoscrolls (NSs) of MoS<sub>2</sub> is obtained in [83] using one drop of ethanol. The NSs are said to have 10 times higher mobility than monolayer MoS<sub>2</sub> and with a 100% yield.

A neuromorphic image sensor based on MoS<sub>2</sub>-organic heterostructure similar to human vision system in [84], showed simple design and better image in case of noisy inputs Figure 3. The idea of the image sensor lies in the quasi-linear time-dependent photocurrent generation and prolonged photocurrent decay, by the trapping effect of MoS<sub>2</sub> stack.

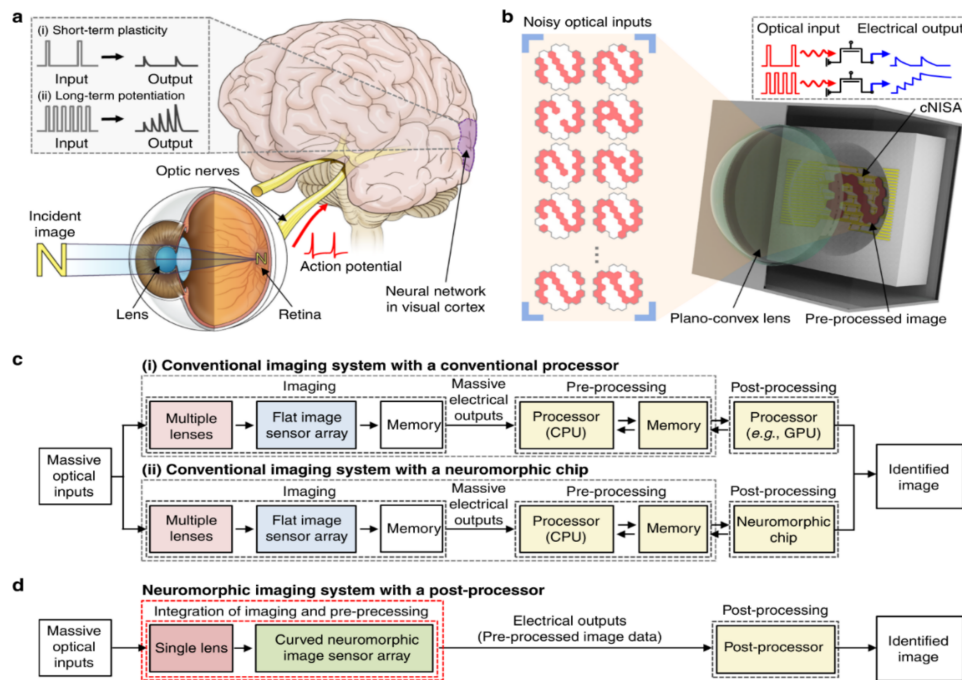


**Figure 3.** Optical application of MoS<sub>2</sub>. Curved neuromorphic imaging device inspired by the human visual recognition system. (a) Human visual recognition system (b) Curved neuromorphic imaging device (c) Block diagram of conventional imaging system (d) Proposed Curved neuromorphic imaging system. Reproduced from [84]. Springer Nature 2020.

#### 4.2. Medical Applications

MoS<sub>2</sub> has a role in diseases' detection and curing, making use of its PL, chemical properties, and biocompatibility. Molybdenum disulfide/graphene oxide (MoS<sub>2</sub>/GO) with doxorubicin (a chemotherapeutic agent) was found to cure lung cancer [85], the nanocomposite showed good results in vitro, and in vivo and was experimented on mice lungs Figure 4. MoS<sub>2</sub>/GO was compared with other complexes (doxorubicin (DOX), Lysine (Lys)-MoS<sub>2</sub>) and it showed best results with GO and DOX. Mo is known to form a linkage with DOX and though serves as a drug delivery. In [20], a biosensor microfluidic device was proposed that detect an avian Coronavirus using 2D MoS<sub>2</sub>. In [86], a MoS<sub>2</sub>/graphene oxide (RGO) Field Effect Transistor Sensor to detect Hydrogen Peroxide (H<sub>2</sub>O<sub>2</sub>) is proposed. H<sub>2</sub>O<sub>2</sub> is a biomarker for many diseases like cancer, and Alzheimer's disease, Figure 5. In [23], MoS<sub>2</sub> nanosheets are used to detect Prostate antigens and in [21], MoS<sub>2</sub> flakes were used as biomarkers for breast cancer based on the PL properties of MoS<sub>2</sub>. Using a bottom-up synthesizing technique and defect engineering in [87], the photodynamic property of MoS<sub>2</sub> quantum dots (QD) was able of killing cancer cells with high efficiency.

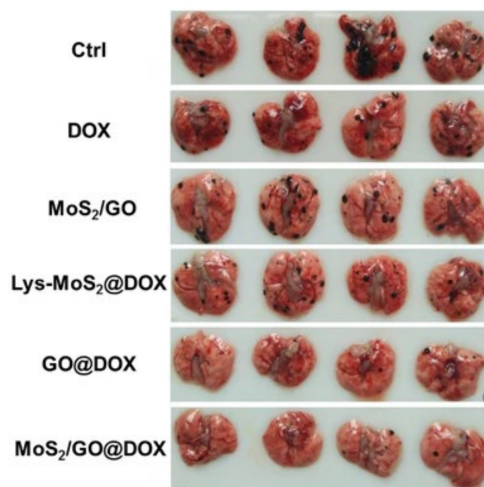


**Figure 4.** The effect of different complexes in killing cancer cells in mice lungs. Adapted from [85]. Springer Nature 2018.

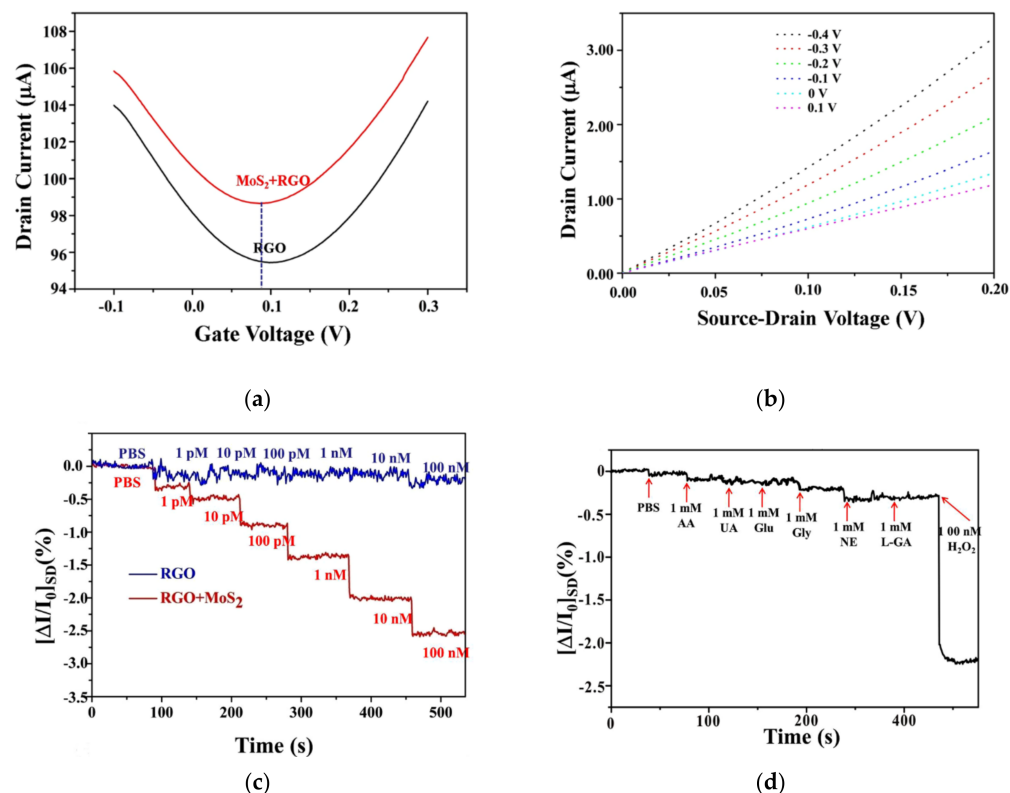


**Figure 5.**  $\text{MoS}_2/\text{RGO}$  FET for detecting  $\text{H}_2\text{O}_2$ , (a) Transfer characteristics for  $\text{MoS}_2/\text{RGO}$  FET, Drain current versus gate voltage for  $\text{MoS}_2/\text{RGO}$  and RGO FETs (b) Drain current versus source-drain voltage for  $\text{MoS}_2/\text{RGO}$ , (c) The change in drain-source current for different concentrations of  $\text{H}_2\text{O}_2$  (d) Negligible current change for different interferents (PBS, 1 mM AA, 1 mM UA, 1 mM Glu, 1 mM GLY, 1 mM NE, 1 mM L-GA) and a noticeable change for  $\text{H}_2\text{O}_2$ . Adapted from [86]. Springer Nature 2019.

$\text{MoS}_2$  has a wide range of applications in microfluidic devices and immunosensors, making use of its chemical and photoluminescence properties [88].  $\text{MoS}_2$  nanosheets were used with microfluidics electrode for detecting *Salmonella typhimurium* (*S.typhimurium*) [89] the proposed device has fast detection and high sensitivity and can be used for other food related pathogens like *E.coli*, Cholera. Depending on the dye-quenching properties of  $\text{MoS}_2$ , its nanosheets were used with microfluidic devices to detect single-stranded DNA (ssDNA),

where MoS<sub>2</sub> showed high fluorescence quenching within few minutes, besides it behaves differently towards ssDNA and double-stranded DNA (dsDNA) where it did not affect the dye of dsDNA [22]. This opens the way for various DNA and diseases' detection, especially cancer. Many diseases like diabetes, digestive disorders and cancer cause a change in the amino acid chain. Amino acids are the building blocks of proteins. The detecting of amino acids is more complex than DNA, since they have 20 bases rather than four in case of DNA and changing their sequence gives different kinds of proteins. Nanopores were recently used in detecting DNA and amino acids, where the amino acid is forced to pass through a nanopore, then the ionic current and the residence time is measured. Each amino acid or DNA has a different ionic current and residence time; however, they are very similar in case of amino acids which make them hard to differentiate. Machine learning techniques are then used to detect the sequence of the amino acids. Biomolecules are easily stuck to MoS<sub>2</sub> so they can be easily detected. They also have better signal to noise ratio. The MoS<sub>2</sub> nanopore with machine learning is used to detect various kinds of amino acids, with high accuracy up to 99.6% and in a very short time (several ps) [90].

An interesting research in [91] used nanohole-enriched MoS<sub>2</sub> (NR-MoS<sub>2</sub>) nanosheets to destroy bacteria and biofilms. The cure is based on the electron transport between NR-MoS<sub>2</sub> and the bacteria, where NR-MoS<sub>2</sub> is a nanosheet of MoS<sub>2</sub> defects and holes. The results were excellent *in vivo* and *vitro* and MoS<sub>2</sub> showed high biocompatibility. The idea behind antimicrobial nanomaterials is that they act as anti-bacterial but without the generation of resistance that happens in typical antibiotics.

#### 4.3. Sensing Applications

The sensing applications of MoS<sub>2</sub> are related, where we can't separate the use of optical, medical, and electronic applications in sensing, but this section summarizes most of the sensing applications reported in the literature. Figure 6 divides the sensing applications into four main categories: biosensing, gas sensing, refractive index sensing, and photo-sensing (photodetectors) [92]. Each application includes different types of sensors, for example, biosensing includes electrochemical sensors, FET based sensors, optical and surface plasmon resonance (SPR) sensors. Both gas sensors [93–96] and photodetectors [72–74] are FET-based sensors. Electrochemical sensing is being studied recently for ultrasensitive sensing, and MoS<sub>2</sub> shows sensitive electrochemical detection properties when combined with other materials where a notable change in the electrochemical impedance occurs. This technique was used in [89] to detect food pathogens.

Based on the fluorescence and quenching properties of MoS<sub>2</sub>, it can be used in biosensing to detect DNA, cancer biomarkers, and different amino acids [21,23,97]. FET-based sensors are also used for biomolecular sensing like DNA, antigens, proteins, biotin, and pH values [97]. Optical sensors are mainly based on the PL characteristics and fluorescence quenching and recovery properties of MoS<sub>2</sub>. It can be used in detecting DNA, H<sub>2</sub>O<sub>2</sub>, and ion sensors.

The SPR biosensors, optical and refractive index biosensors are all related. SPR sensors are based on an optical technique that urges the emission of electromagnetic waves (plasmons). The propagation of plasmons over the material surface is very sensitive to any refractive index change on the surface, and though can detect thin films on the surface [98]. MoS<sub>2</sub> is used with other materials in a SPR sensor to enhance sensitivity to 101.42 °/RIU [99]. It shows a polarization-dependent optical absorption that can be integrated in waveguides to sense refractive index [100]. Table 4 gives a summary of the sensing applications along with the MoS<sub>2</sub> property that enables such sensing.

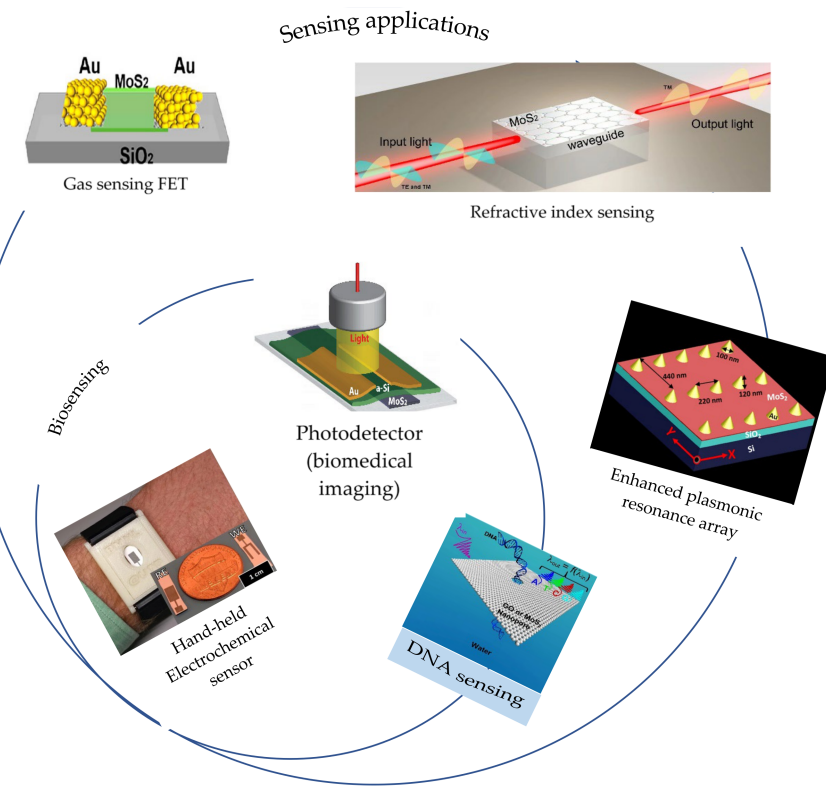


**Figure 6.** Illustrative diagram of different sensing applications of MoS<sub>2</sub>. Enhanced plasmonic resonance array [101], DNA sensing using MoS<sub>2</sub> nanopores [88,102], photodetector for biomedical imaging [72], refractive index sensing [100], gas sensing FET [103], Electrochemical biosensor for measuring cortisol in human sweat [104].

**Table 4.** Summary of sensing applications.

Category	Application	MoS <sub>2</sub> Property	Reference
Optoelectronics	Photosensing (photodetector)	Electronic and optical properties	[72]
	Photosensing (photodetector)		[73]
	Photosensing (photodetector)		[74]
Recognition systems and IoT	Image sensors	Optical properties	[84]
Medical (bio-sensing)	Cancer sensing	PL property	[86]
	Cancer sensing	PL property	[23]
	Cancer sensing	PL property	[21]
	DNA sensing	MoS <sub>2</sub> nanopores	[88]
	DNA sensing	dye quenching property	[97]
	Amino acids sensing	MoS <sub>2</sub> nanopores	[90]
	Immunosensors	Electrochemical and optical properties	[89]

#### 4.4. Miscellaneous Applications

MoS<sub>2</sub> has terahertz and microwave applications [105,106] where a tunable terahertz wave reflector made of MoS<sub>2</sub>, SiO<sub>2</sub>, gold was proposed in [107]. The proposed structure enhances the design of beam manipulation devices and can be used in THz radiation control [108] as an alternative to complex antenna structures [109–114]. A terahertz modulator

based on MoS<sub>2</sub> on Silicon was presented in [115], with higher modulation efficiency when compared to graphene-based devices.

It is used in hydrogen detection [116] and generation [117] (hydrogen evolution reactions HER). Hydrogen production is one of the demanded industries due to its low toxicity and its use in many important fields like the fuel industry [118] and essential chemical processes. MoS<sub>2</sub> represents a cheap electrochemical hydrogen generation method [119], and it is said to substitute platinum-based catalysts in hydrogen generation processes. The strategy used was based on synthesizing edge-terminated MoS<sub>2</sub> nanosheets with wide interlayer spacing under microwave heating technique. The work presents a new catalyst design concept. It also has a role in Oxygen evolution reactions (OER) and CO<sub>2</sub> reduction where it reduces it to CO [120].

MoS<sub>2</sub> has a role in recent environmental issues like adsorption of Organic Contaminants [121], and oil-water separation [122]. In water separation, MoS<sub>2</sub> nanosheets were used to develop a sponge for oil-water separation. MoS<sub>2</sub> has a strong hydrophobicity property that it absorbs other organic solvents with high selectivity. Table 5. provides a comprehensive list of the reported MoS<sub>2</sub> applications with the field of interest.

**Table 5.** Summary of MoS<sub>2</sub> application.

Application	Category	Description	Publisher	Year	Reference
Electronics	Analogue	Developing a 2D MoS <sub>2</sub> field-effect transistors (FETs) to be used as operational amplifier	Nature	2020	[71]
Electronics	CMOS	Enhanced back gate MoS <sub>2</sub> FETs using Sulfur treatment, gate length from 500 to 80 nm, contact resistance = 1.3 kΩ	IEEE	2020	[75]
Electronics	nonvolatile memory	Hystresses and capacitance of MoS <sub>2</sub> NVM with 9nm and 15 nm blocking oxide layer of SiO <sub>2</sub> is investigated. The device has largest hystresses window. And can store both electrons and holes	IEEE	2016	[77]
Electronics	Power electronics	Ultra low power transistor of SS ~4.5 mm/decade and steep on/off characteristics	Nature	2020	[76]
Electronics	optoelectronics	Developing a highly-efficient and fast photodetector using amorphous silicon and MoS <sub>2</sub>	Nature	2013	[72]
Electronics	optoelectronics	Efficient photodetector with photocurrent gain of 1.6, specific detectivity of $4.32 \times 10^8$ Jones and quantum efficiency $\sim 1.0 \times 10^{10}$ at 365 nm	Nature	2020	[73]
Electronics	optoelectronics	A nanoscale photodetector, energy efficient (consumes from 1 to 1000 nanojoules), and has a small fingerprint of ( $\sim 1 \mu\text{m} \times 5 \mu\text{m}$ ). A MoS <sub>2</sub> -organic heterostructure image sensor similar to human vision system using simple design. The output has less noise and without redundant input data	Nature	2020	[74]
Electronics	Image sensors	similar to human vision system using simple design. The output has less noise and without redundant input data	Nature	2020	[84]
Medical	Cancer cure	Using MoS <sub>2</sub> /GO nanocomposites to cure lung cancer in mice	Nature	2018	[85]
Medical	Cancer cure	Using defect engineering (Sulfur defects) in MoS <sub>2</sub> quantum dots to kill cancer cells. The Sulfur defects increased oxidation strees and was able to inhibit cancer growth cells	Nature	2019	[87]
Medical	Cancer detection	A real-time MoS <sub>2</sub> FET sensor to detect H <sub>2</sub> O <sub>2</sub> in biological cells	Nature	2019	[86]

**Table 5.** *Cont.*

Application	Category	Description	Publisher	Year	Reference
Medical	Cancer detection	MoS <sub>2</sub> nanosheet fluorescent biosensor for detecting prostate antigen. A 20 µg/mL of MoS <sub>2</sub> nanosheets quenched up to 97% of the dye	Springer	2014	[23]
Medical	Cancer detection	Detecting breast cancer based on PL property of MoS <sub>2</sub> . A redshift of 16 nm takes place for miRNA21c (a cancer biomarker)	Nature	2020	[21]
Medical	DNA detection	Sensing DNA nucleobases using MoS <sub>2</sub> nanopores. Molar absorption of MoS <sub>2</sub> nanopore of 0.65 nm thick, and lengths 2 nm, 3 nm, 5 nm.	Nature	2019	[88]
Medical	DNA detection	Detecting DNA based on dye quenching property of MoS <sub>2</sub> . The device has linear range (0 to 50 nM), and a detection limit = 500 pM	Royal Society of chemistry	2015	[97]
Medical	Amino acid detection	Using MoS <sub>2</sub> nanopores and machine learning to detect ionic current and residence time of 20 different amino acids with accuracy range 72.45% to 99.6%	Nature	2018	[90]
Medical	Microfluidic immunosensor	Use of MoS <sub>2</sub> nanosheets on microfluidic electrodes to detect <i>Salmonella typhimurium</i> ( <i>S.typhimurium</i> ) sensitivity = 1.79 kΩ/(CFU/mL.cm <sup>2</sup> ) detection limit = 1.56 CFU/mL detection range = 10–10 <sup>7</sup> CFU/mL.	Elsevier	2017	[89]
Medical	Antibacterial materials	Using nanohole enriched MoS <sub>2</sub> to destroy bacteria. MoS <sub>2</sub> concentration used is 4 µg/mL. It has affinity response with biofilms of 14.71 nM, 1.3-fold > 11.44 nM obtained for pristine MoS <sub>2</sub> Verified in vitro and viro	Nature	2021	[91]
Energy	Solar cells	Using MoS <sub>2</sub> as a buffer in solar cells to enhance efficiency and stability	IEEE	2016	[123]
Energy	Solar cells	Using MoS <sub>2</sub> as a hole transport layer in solar cells a peak at 404 cm <sup>-1</sup> , at 200 °C, and two more peaks at at 380 and 404 cm <sup>-1</sup> , at 300 °C,	Wiley	2019	[124]

**Table 5.** *Cont.*

Application	Category	Description	Publisher	Year	Reference
Energy	Solar cells	MoS <sub>2</sub> as a transport layer in perovskite solar cells PCE ( $\eta$ ) = 3.9% compared to other cells of ( $\eta$ = 3.1%). High stability for 800-hour shelf life ( $\Delta$ PCE/PCE = -17%) when compared to other cells of ( $\Delta$ PCE/PCE = -45%).	IEEE	2015	[125]
Energy	Solar cells	Using MoS <sub>2</sub> /Si heterojunction in solar cells to enhance conversion efficiency from 1.1% to 4.6%.	Elsevier	2018	[126]
Energy	Solar cells	Enhancing organometallic-halide perovskite solar using MoS <sub>2</sub> as a buffer Cells (PCE) = 14.9%, and maintaining 93.1% of its PCE after 1 hour	Nature	2020	[127]
Energy	lithium-ion batteries	Using MoS <sub>2</sub> as anode material for lithium-ion batteries. It has capacity of 1103.6 mAh/g and maintains a reversible capacity of 786.4 mAh/g after 50 cycles at 0.1 A/g	Elsevier	2019	[128]
THz applications	THz wave reflector	Switchable THz wave reflector made of MoS <sub>2</sub> , SiO <sub>2</sub> , and gold layers. reflection phase ranges from 0 to $2\pi$ linear phase shift according to the geometric dimension	IEEE	2018	[107]
THz applications	THz modulator	Terahertz modulator of multilayer-MoS <sub>2</sub> on Silicon (MOS). Modulation efficiency of annealed MOS is higher than that of graphene over Silicon and graphene metamaterials	Nature	2016	[115]
Other	Hydrogen detection	MoS <sub>2</sub> -PVP (Polyvinyl pyridine) nanocomposite with ZnO to detect hydrogen. A 5 mg/mL sensor has 8 times better sensing than pristine ZnO coordination polymer based on [Mo <sub>3</sub> S <sub>13</sub> ] <sup>2-</sup> clusters from amorphous MoS <sub>2</sub> to be used in hydrogen evolution reactions.	IEEE	2021	[116]
Other	Hydrogen generation	A edge-terminated and interlayer-expanded MoS <sub>2</sub> catalyst fabricated using a microwave heating strategy. The proposed structure has the highest hydrogen evolution activity and best stability	Nature	2016	[117]
Other	Hydrogen generation	MoS <sub>2</sub> Sponge to absorb oil from water. Simple fabrication and easy scaling up.	Nature	2015	[118]
Other	Oil separation from water		Nature	2016	[122]

## 5. Challenges

Molybdenum disulfide material is still under study, although it has favorable chemical, photonic, and electronic characteristics, there are still more to be done regarding its way of preparation and compatibility with other materials, as summarized in Figure 7.



**Figure 7.** Illustrative diagram of challenges facing MoS<sub>2</sub>.

Although MoS<sub>2</sub> showed acceptable electronic characteristics, it has less mobility (30–60 cm<sup>2</sup>/Vs) and higher band gap (1.8 eV) than Silicon (~1000 cm<sup>2</sup>/Vs and 1.1eV) [129–131]. MoS<sub>2</sub> FETs have some issues with mobility, electro-statistics and strain below 6.6 nm gate lengths [132], which means we cannot achieve the required sub 10 nm International Technology Road Map (ITRS). We are still facing challenges in synthesizing techniques for the production of different 2D structures that are hard to separate. Moreover, the stability of MoS<sub>2</sub> against moisture, humidity, and other environmental conditions needs more study [133].

The researchers in [134] studied the effect of impurities and atomic vacancies of Mo and S in MoS<sub>2</sub> structure. The absence of Mo or S and especially Mo vacancy leads to gap states that result in a noticeable current at low voltage biasing. Atomic vacancies affect the electron and hole transport of MoS<sub>2</sub>.

MoS<sub>2</sub> layers like other 2D materials are prone to laser damage when used as optical modulators [135]. The fast response of these materials transfers a remarkable portion of light into heat that can result in complete damage or burn to the material. Additionally, MoS<sub>2</sub> structure has some defects that cause performance degradation and low reliability when used in device applications. As an example, MoS<sub>2</sub> layers fabricated through CVD have many dangling bonds and high reactivity. The grain boundaries and point defects were studied in [136], while those studies are references to control MoS<sub>2</sub> defects and other TMDs using defect engineering methods.

More studies are needed for the lattice mismatch that occurs between monolayers. The mismatch cause band gap moiré and affect spectroscopy of MoS<sub>2</sub> bilayer [137].

Although MoS<sub>2</sub> has mechanical flexibility and strength that facilitates its strain engineering, the material exhibits nonuniform strain distribution. This happens because of the large number of atoms involved under strain which needs further study [138,139]. The non-equilibrium in MoS<sub>2</sub> structure is related to the temperature and the heating rate applied during synthesizing [140], which calls for new synthesizing methods.

Although MoS<sub>2</sub> is said to have good biocompatibility, bio absorbability, cancer killing, and anti-bacterial effect, a very important research published in Nature in 2018 states a highly toxic effect of MoS<sub>2</sub> nanosheets [141]. MoS<sub>2</sub> were investigated to induce cytotoxic effect and cell damage when interacting with tumor cells, while no effect in case of normal cells. The cytotoxic effect depends on the concentration and number of layers of MoS<sub>2</sub> that can be manipulated in the future. The nano- and micro- MoS<sub>2</sub> sheets showed a change in the metabolic profiles on the intestine of mice [142]. Also nano-MoS<sub>2</sub> sheets showed greater intestine inflammation. Both changed the intestinal microbiota. Table 6 provides a summary of the reported challenges facing MoS<sub>2</sub> in the literature, and their types.

**Table 6.** Summary of challenges facing MoS<sub>2</sub>.

Challenge	Description	Publisher	Year	Reference
Properties	Effect of lattice imperfections and atomic vacancies on density of states and electron-hole transport	IEEE	2015	[134]
Properties	Degradation behavior of MoS <sub>2</sub> crystals	NPG Asia Materials	2018	[136]
Properties	structural transformations in MoS <sub>2</sub> thin layers under high temperature	Nature	2020	[140]
Electronics	Sub 10 nm FETs challenges and Strain effects	IEEE	2015	[132]
Optoelectronics	Optical modulation challenges and laser damage	Advanced Materials	2017	[135]
Optoelectronics	optical spectroscopy for MoS <sub>2</sub> layers, the absorption and emission behavior and how to tune them	Nature	2021	[137]
Optoelectronics	Strain engineering to develop optical properties and using it in photonics applications	Nature	2020	[138]
Optoelectronics	Failure mechanisms of monolayer MoS <sub>2</sub> under large strain	Journal of physics	2015	[139]
Biomedical (biocompatibility)	Cytotoxic effect of MoS <sub>2</sub> when used to cure cancer cells	Nature	2018	[141]
Biomedical (biocompatibility)	Effect of nano-MoS <sub>2</sub> on mice intestine where it caused intestinal inflation and changes in the metabolism and the microbiota	Royal Society of chemistry	2019	[142]

## 6. Conclusions

In this review, we highlighted the different MoS<sub>2</sub> structures and their synthesizing techniques in detail, and we provided a comprehensive comparison between all the structures, in term of their main optical, lattice and electrical properties and applications. Synthesis techniques were also covered with their main advantages and inconveniences. A review of the wide range applications of MoS<sub>2</sub> from electronics, medicine to new fields of research such as the terahertz field and the hydrogen-related technologies was made. We also discussed and compared the different challenges facing the development of MoS<sub>2</sub> applications in different fields of study, since they were not discussed in detail in previous studies that focused more on synthesizing techniques or specific kinds of applications.

MoS<sub>2</sub> is a promising material with a wide range of applications. Its outstanding properties and band gap characteristics allowed its use in biosensing, electronics, optoelectronics, and energy applications. It has good biocompatibility and bio absorbability

that allowed its use in several diseases' curing like cancer, Alzheimer, and Coronavirus. Its photoluminescence properties helped in DNA detection. It is believed that MoS<sub>2</sub> can substitute Silicon semiconductor devices. On the other hand, there are some challenges facing MoS<sub>2</sub> that needs to be studied, like managing its impurities, lattice imperfections, and finding the best way of synthesizing that guarantees the largest yield, the cheapest cost, and the highest quality without changing its chemical and physical properties.

In a summary, this review provides an understanding of the major challenges facing the development of MoS<sub>2</sub>-based solutions, especially in the untapped new fields of applications. The integration of MoS<sub>2</sub> with other 2D nanomaterials, such as graphene, in hybrid structures can provide a tradeoff between the shortcomings of both materials and a better combination of their main advantages to overcome the existing challenges.

**Author Contributions:** Conceptualization, O.S. and A.E.M.; methodology, O.S. and A.E.M.; writing—original draft preparation, O.S. and A.E.M.; writing—review and editing, M.D.B., S.Z., and A.E.M.; supervision, A.E.M. All authors have read and agreed to the published version of the manuscript.

**Funding:** This research was funded by United Arab Emirates University UPAR project, grant number 31N393.

**Institutional Review Board Statement:** Not applicable.

**Informed Consent Statement:** Not applicable.

**Data Availability Statement:** Not applicable.

**Conflicts of Interest:** The authors declare no conflict of interest.

## References

- He, Z.; Que, W. Molybdenum Disulfide Nanomaterials: Structures, Properties, Synthesis and Recent Progress on Hydrogen Evolution Reaction. *Appl. Mater. Today* **2016**, *3*, 23–56. [[CrossRef](#)]
- Hersam, M.C. Emerging Device Applications for Two-Dimensional Nanomaterial Heterostructures. In Proceedings of the 2015 73rd Annual Device Research Conference (DRC), Columbus, OH, USA, 21–24 June 2015; IEEE: Columbus, OH, USA, 2015; p. 209.
- Zhao, G.-Y.; Deng, H.; Tyree, N.; Guy, M.; Lisfi, A.; Peng, Q.; Yan, J.-A.; Wang, C.; Lan, Y. Recent Progress on Irradiation-Induced Defect Engineering of Two-Dimensional 2H-MoS<sub>2</sub> Few Layers. *Appl. Sci.* **2019**, *9*, 678. [[CrossRef](#)]
- Del Alamo, J.A. Nanometre-Scale Electronics with III-V Compound Semiconductors. *Nature* **2011**, *479*, 317–323. [[CrossRef](#)] [[PubMed](#)]
- Geim, A.K.; Grigorieva, I.V. Van Der Waals Heterostructures. *Nature* **2013**, *499*, 419–425. [[CrossRef](#)]
- Current, M.I. Process and Metrology Challenges for Nano-Scale Electronics. In Proceedings of the 2016 IEEE Workshop on Microelectronics and Electron Devices (WMED), Boise, ID, USA, 15 April 2016; IEEE: Boise, ID, USA, 2016; pp. 1–5.
- Butler, S.Z.; Hollen, S.M.; Cao, L.; Cui, Y.; Gupta, J.A.; Gutiérrez, H.R.; Heinz, T.F.; Hong, S.S.; Huang, J.; Ismach, A.F.; et al. Progress, Challenges, and Opportunities in Two-Dimensional Materials Beyond Graphene. *ACS Nano* **2013**, *7*, 2898–2926. [[CrossRef](#)]
- Bhat, N. Tunable Steep Slope MoS<sub>2</sub> Transistor. In Proceedings of the 2018 IEEE International Conference on Semiconductor Electronics (ICSE), Kuala Lumpur, Malaysia, 15–17 August 2018; IEEE: Kuala Lumpur, 2018; p. C1.
- Novoselov, K. Beyond the Wonder Material. *Phys. World* **2009**, *22*, 27–30. [[CrossRef](#)]
- Moutaoukil, A.E.; Kang, H.-C.; Handa, H.; Fukidome, H.; Suemitsu, T.; Sano, E.; Suemitsu, M.; Otsuji, T. Room Temperature Logic Inverter on Epitaxial Graphene-on-Silicon Device. *Jpn. J. Appl. Phys.* **2011**, *50*, 070113. [[CrossRef](#)]
- Yoo, G.; Lee, S.; Yoo, B.; Han, C.; Kim, S.; Oh, M.S. Electrical Contact Analysis of Multilayer MoS<sub>2</sub> Transistor With Molybdenum Source/Drain Electrodes. *IEEE Electron Device Lett.* **2015**, *36*, 1215–1218. [[CrossRef](#)]
- Das, S. 2D Materials for Ubiquitous Electronics. In Proceedings of the 2018 IEEE 2nd Electron Devices Technology and Manufacturing Conference (EDTM), Kobe, Japan, 13–16 March 2018; IEEE: Kobe, Japan, 2018; pp. 19–20.
- Hiraki, A. Recent Developments on Metal-Silicon Interfaces. *Appl. Surf. Sci.* **1992**, *56–58*, 370–381. [[CrossRef](#)]
- Desai, S.B.; Madhvapathy, S.R.; Sachid, A.B.; Llinas, J.P.; Wang, Q.; Ahn, G.H.; Pitner, G.; Kim, M.J.; Bokor, J.; Hu, C.; et al. MoS<sub>2</sub> Transistors with 1-Nanometer Gate Lengths. *Science* **2016**, *354*, 99–102. [[CrossRef](#)]
- Hoefflinger, B. Nanolithography. In *NANO-CHIPS 2030: On-Chip AI for an Efficient Data-Driven World*; Murmann, B., Hoefflinger, B., Eds.; The Frontiers Collection; Springer International Publishing: Stanford, CA, USA, 2020; pp. 41–45. ISBN 978-3-030-18338-7.
- International Roadmap for Devices and Systems (IRDS™) 2020 Edition-IEEE IRDS™. Available online: <https://irds.ieee.org/editions/2020> (accessed on 10 March 2021).
- Iwai, H.; Kakushima, K.; Wong, H. Challenges for future semiconductor manufacturing. *Int. J. High Speed Electron. Syst.* **2006**, *16*, 43–81. [[CrossRef](#)]

18. Irtegov, Y.; An, V.; Azhgikhin, M. Study of Nanostructured Metal Sulfides Produced by Self-Propagating High-Temperature Synthesis. In Proceedings of the 2012 7th International Forum on Strategic Technology (IFOST), Tomsk, Russia, 18–21 September 2012; IEEE: Tomsk, Russia, 2012; pp. 1–4.
19. Sha, J.; Xu, W.; Yuan, Z.; Xu, B.; Chen, Y. Fabrication of Liquid-Gated Molybdenum Disulfide Field-Effect Transistor. In Proceedings of the 2017 IEEE 12th International Conference on Nano/Micro Engineered and Molecular Systems (NEMS), Los Angeles, CA, USA, 9–12 April 2017; IEEE: Los Angeles, CA, USA, 2017; pp. 788–791.
20. Weng, X.; Neethirajan, S. Immunosensor Based on Antibody-Functionalized MoS<sub>2</sub> for Rapid Detection of Avian Coronavirus on Cotton Thread. *IEEE Sens. J.* **2018**, *18*, 4358–4363. [CrossRef]
21. Catalán-Gómez, S.; Briones, M.; Cortijo-Campos, S.; García-Mendiola, T.; de Andrés, A.; Garg, S.; Kung, P.; Lorenzo, E.; Pau, J.L.; Redondo-Cubero, A. Breast Cancer Biomarker Detection through the Photoluminescence of Epitaxial Monolayer MoS<sub>2</sub> Flakes. *Sci. Rep.* **2020**, *10*, 16039. [CrossRef]
22. Liu, Y.; Zhang, J.; Shen, Y.; Yan, J.; Hou, Z.; Mao, C. MoS<sub>2</sub> quantum dots featured fluorescent biosensor for multiple detection of cancer. *RSC Adv.* **2017**, *7*, 54638–54643. [CrossRef]
23. Kong, R.-M.; Ding, L.; Wang, Z.; You, J.; Qu, F. A Novel Aptamer-Functionalized MoS<sub>2</sub> Nanosheet Fluorescent Biosensor for Sensitive Detection of Prostate Specific Antigen. *Anal. Bioanal. Chem.* **2015**, *407*, 369–377. [CrossRef]
24. Sobanska, Z.; Zapor, L.; Szparaga, M.; Stepnik, M. Biological Effects of Molybdenum Compounds in Nanosized Forms under in Vitro and in Vivo Conditions. *Int. J. Occup. Med. Environ. Health* **2020**, *33*, 1–19. [CrossRef]
25. Hossain, R.F.; Deaguero, I.G.; Boland, T.; Kaul, A.B. Biocompatible, Large-Format, Inkjet Printed Heterostructure MoS<sub>2</sub>-Graphene Photodetectors on Conformable Substrates. *NPJ 2D Mater. Appl.* **2017**, *1*, 28. [CrossRef]
26. Liu, L.; Liu, Z.; Huang, P.; Wu, Z.; Jiang, S. Protein-Induced Ultrathin Molybdenum Disulfide (MoS<sub>2</sub>) Flakes for a Water-Based Lubricating System. *RSC Adv.* **2016**, *6*, 113315–113321. [CrossRef]
27. Gupta, D.; Chauhan, V.; Kumar, R. A Comprehensive Review on Synthesis and Applications of Molybdenum Disulfide (MoS<sub>2</sub>) Material: Past and Recent Developments. *Inorg. Chem. Commun.* **2020**, *121*, 108200. [CrossRef]
28. Li, X.; Zhu, H. Two-Dimensional MoS<sub>2</sub>: Properties, Preparation, and Applications. *J. Mater.* **2015**, *1*, 33–44. [CrossRef]
29. Yadav, V.; Roy, S.; Singh, P.; Khan, Z.; Jaiswal, A. 2D MoS<sub>2</sub>-Based Nanomaterials for Therapeutic, Bioimaging, and Biosensing Applications. *Small* **2019**, *15*, 1803706. [CrossRef]
30. Chodankar, N.R.; Nanjundan, A.K.; Losic, D.; Dubal, D.P.; Baek, J.-B. Graphene and Molybdenum Disulphide Hybrids for Energy Applications: An Update. *Mater. Today Adv.* **2020**, *6*, 100053. [CrossRef]
31. Winer, W.O. Molybdenum Disulfide as a Lubricant: A Review of the Fundamental Knowledge. *Wear* **1967**, *10*, 422–452. [CrossRef]
32. Jiao, Y.; Hafez, A.M.; Cao, D.; Mukhopadhyay, A.; Ma, Y.; Zhu, H. Metallic MoS<sub>2</sub> for High Performance Energy Storage and Energy Conversion. *Small* **2018**, *14*, 1800640. [CrossRef]
33. Toh, R.J.; Sofer, Z.; Luxa, J.; Sedmidubský, D.; Pumera, M. 3R Phase of MoS<sub>2</sub> and WS<sub>2</sub> Outperforms the Corresponding 2H Phase for Hydrogen Evolution. *Chem. Commun.* **2017**, *53*, 3054–3057. [CrossRef]
34. Krishnan, U.; Kaur, M.; Singh, K.; Kumar, M.; Kumar, A. A Synoptic Review of MoS<sub>2</sub>: Synthesis to Applications. *Superlattices Microstruct.* **2019**, *128*, 274–297. [CrossRef]
35. Manzeli, S.; Dumcenco, D.; Migliato Marega, G.; Kis, A. Self-Sensing, Tunable Monolayer MoS<sub>2</sub> Nanoelectromechanical Resonators. *Nat. Commun.* **2019**, *10*, 4831. [CrossRef]
36. Cao, J.; Zhou, J.; Chen, J.; Wang, W.; Zhang, Y.; Liu, X. Effects of Phase Selection on Gas-Sensing Performance of MoS<sub>2</sub> and WS<sub>2</sub> Substrates. *ACS Omega* **2020**, *5*, 28823–28830. [CrossRef]
37. Dai, Z.; Jin, W.; Grady, M.; Sadowski, J.T.; Dadap, J.I.; Osgood, R.M.; Pohl, K. Surface Structure of Bulk 2H-MoS<sub>2</sub>(0001) and Exfoliated Suspended Monolayer MoS<sub>2</sub>: A Selected Area Low Energy Electron Diffraction Study. *Surf. Sci.* **2017**, *660*, 16–21. [CrossRef]
38. Siao, M.D.; Shen, W.C.; Chen, R.S.; Chang, Z.W.; Shih, M.C.; Chiu, Y.P.; Cheng, C.-M. Two-Dimensional Electronic Transport and Surface Electron Accumulation in MoS<sub>2</sub>. *Nat. Commun.* **2018**, *9*, 1442. [CrossRef] [PubMed]
39. Venkata Subbaiah, Y.P.; Saji, K.J.; Tiwari, A. Atomically Thin MoS<sub>2</sub>: A Versatile Nongraphene 2D Material. *Adv. Funct. Mater.* **2016**, *26*, 2046–2069. [CrossRef]
40. Seivane, L.F.; Barron, H.; Botti, S.; Lopes Marques, M.A.; Rubio, Á.; López-Lozano, X. Atomic and Electronic Properties of Quasi-One-Dimensional MoS<sub>2</sub> Nanowires. *J. Mater. Res.* **2013**, *28*, 240–249. [CrossRef] [PubMed]
41. Elizondo-Villarreal, N.; Velázquez-Castillo, R.; Galván, D.H.; Camacho, A.; José Yacamán, M. Structure and Catalytic Properties of Molybdenum Sulfide Nanoplatelets. *Appl. Catal. A Gen.* **2007**, *328*, 88–97. [CrossRef]
42. Saleem, U.; Permatasari, F.A.; Iskandar, F.; Ogi, T.; Okuyama, K.; Darma, Y.; Zhao, M.; Loh, K.P.; Rusydi, A.; Coquet, P.; et al. Surface Plasmon Enhanced Nitrogen-Doped Graphene Quantum Dot Emission by Single Bismuth Telluride Nanoplates. *Adv. Opt. Mater.* **2017**, *5*, 1700176. [CrossRef]
43. Tahersima, M.H.; Birowosuto, M.D.; Ma, Z.; Coley, W.C.; Valentin, M.D.; Naghibi Alvillar, S.; Lu, I.-H.; Zhou, Y.; Sarpkaya, I.; Martinez, A.; et al. Testbeds for Transition Metal Dichalcogenide Photonics: Efficacy of Light Emission Enhancement in Monomer vs Dimer Nanoscale Antennae. *ACS Photonics* **2017**, *4*, 1713–1721. [CrossRef]
44. Hou, S.; Tobing, L.Y.M.; Wang, X.; Xie, Z.; Yu, J.; Zhou, J.; Zhang, D.; Dang, C.; Coquet, P.; Tay, B.K.; et al. Manipulating Coherent Light–Matter Interaction: Continuous Transition between Strong Coupling and Weak Coupling in MoS<sub>2</sub> Monolayer Coupled with Plasmonic Nanocavities. *Adv. Opt. Mater.* **2019**, *7*, 1900857. [CrossRef]

45. Halim, S.N.M.; Zuikafly, S.N.F.; Taib, M.F.M.; Ahmad, F. First Principles Study on Electronic and Optical Properties of Graphene/MoS<sub>2</sub> for Optoelectronic Application. In Proceedings of the 2020 IEEE International Conference on Semiconductor Electronics (ICSE), Kuala Lumpur, Malaysia, 28–29 July 2020; IEEE: Kuala Lumpur, Malaysia, 2020; pp. 29–32.
46. Nalwa, H.S. A Review of Molybdenum Disulfide (MoS<sub>2</sub>) Based Photodetectors: From Ultra-Broadband, Self-Powered to Flexible Devices. *RSC Adv.* **2020**, *10*, 30529–30602. [[CrossRef](#)]
47. Cheng, Y.; Wang, J.-Z.; Wei, X.-X.; Guo, D.; Wu, B.; Yu, L.-W.; Wang, X.-R.; Shi, Y. Tuning Photoluminescence Performance of Monolayer MoS<sub>2</sub> via H<sub>2</sub>O<sub>2</sub> Aqueous Solution. *Chin. Phys. Lett.* **2015**, *32*, 117801. [[CrossRef](#)]
48. Amani, M.; Lien, D.-H.; Kiriya, D.; Xiao, J.; Azcatl, A.; Noh, J.; Madhvapathy, S.R.; Addou, R.; Kc, S.; Dubey, M.; et al. Near-Unity Photoluminescence Quantum Yield in MoS<sub>2</sub>. *Science* **2015**, *350*, 1065–1068. [[CrossRef](#)]
49. Ghorbani-Asl, M.; Zibouche, N.; Wahiduzzaman, M.; Oliveira, A.F.; Kuc, A.; Heine, T. Electromechanics in MoS<sub>2</sub> and WS<sub>2</sub>: Nanotubes vs. Monolayers. *Sci. Rep.* **2013**, *3*, 2961. [[CrossRef](#)]
50. Johari, P.; Shenoy, V.B. Tuning the Electronic Properties of Semiconducting Transition Metal Dichalcogenides by Applying Mechanical Strains. *ACS Nano* **2012**, *6*, 5449–5456. [[CrossRef](#)]
51. Kadantsev, E.S.; Hawrylak, P. Electronic Structure of a Single MoS<sub>2</sub> Monolayer. *Solid State Commun.* **2012**, *152*, 909–913. [[CrossRef](#)]
52. Tsai, Y.-C.; Li, Y. Impact of Doping Concentration on Electronic Properties of Transition Metal-Doped Monolayer Molybdenum Disulfide. *IEEE Trans. Electron Devices* **2018**, *65*, 733–738. [[CrossRef](#)]
53. Guguchia, Z.; Kerelsky, A.; Edelberg, D.; Banerjee, S.; von Rohr, F.; Scullion, D.; Augustin, M.; Scully, M.; Rhodes, D.A.; Shermadini, Z.; et al. Magnetism in Semiconducting Molybdenum Dichalcogenides. *Sci. Adv.* **2018**, *4*, eaat3672. [[CrossRef](#)]
54. Liang, S. Electrical Spin Injection and Detection in Molybdenum Disulfide Multilayer Channel. *Nat. Commun.* **2019**, *8*, 9. [[CrossRef](#)]
55. Coogan, Á.; Gun’ko, Y.K. Solution-Based “Bottom-up” Synthesis of Group VI Transition Metal Dichalcogenides and Their Applications. *Mater. Adv.* **2021**, *2*, 146–164. [[CrossRef](#)]
56. Sun, J.; Li, X.; Guo, W.; Zhao, M.; Fan, X.; Dong, Y.; Xu, C.; Deng, J.; Fu, Y. Synthesis Methods of Two-Dimensional MoS<sub>2</sub>: A Brief Review. *Crystals* **2017**, *7*, 198. [[CrossRef](#)]
57. Li, M.-Y.; Chen, C.-H.; Shi, Y.; Li, L.-J. Heterostructures Based on Two-Dimensional Layered Materials and Their Potential Applications. *Mater. Today* **2016**, *19*, 322–335. [[CrossRef](#)]
58. Crane, M.J.; Lim, M.B.; Zhou, X.; Pauzauskie, P.J. Rapid Synthesis of Transition Metal Dichalcogenide–Carbon Aerogel Composites for Supercapacitor Electrodes. *Microsyst. Nanoeng.* **2017**, *3*, 17032. [[CrossRef](#)]
59. Vignesh; Kaushik, S.; Tiwari, U.K.; Kant Choubey, R.; Singh, K.; Sinha, R.K. Study of Sonication Assisted Synthesis of Molybdenum Disulfide (MoS<sub>2</sub>) Nanosheets. *Mater. Today: Proc.* **2020**, *21*, 1969–1975. [[CrossRef](#)]
60. Han, J.T.; Jang, J.I.; Kim, H.; Hwang, J.Y.; Yoo, H.K.; Woo, J.S.; Choi, S.; Kim, H.Y.; Jeong, H.J.; Jeong, S.Y.; et al. Extremely Efficient Liquid Exfoliation and Dispersion of Layered Materials by Unusual Acoustic Cavitation. *Sci. Rep.* **2015**, *4*, 5133. [[CrossRef](#)] [[PubMed](#)]
61. Tan, X.; Kang, W.; Liu, J.; Zhang, C. Synergistic Exfoliation of MoS<sub>2</sub> by Ultrasound Sonication in a Supercritical Fluid Based Complex Solvent. *Nanoscale Res. Lett.* **2019**, *14*, 317. [[CrossRef](#)] [[PubMed](#)]
62. Vishwanath, S.; Liu, X.; Rouvimov, S.; Mende, P.C.; Azcatl, A.; McDonnell, S.; Wallace, R.M.; Feenstra, R.M.; Furdyna, J.K.; Jena, D.; et al. Comprehensive Structural and Optical Characterization of MBE Grown MoSe<sub>2</sub> on Graphite, CaF<sub>2</sub> and Graphene. *2D Mater.* **2015**, *2*, 024007. [[CrossRef](#)]
63. Aliofkazraei, M.; Ali, N. PVD Technology in Fabrication of Micro- and Nanostructured Coatings. In *Comprehensive Materials Processing*; Elsevier: Amsterdam, The Netherlands, 2014; pp. 49–84. ISBN 978-0-08-096533-8.
64. Wang, F. Hydrothermal Synthesis of Flower-like Molybdenum Disulfide Microspheres and Their Application in Electrochemical Supercapacitors. *RSC Adv.* **2018**, 1–10. [[CrossRef](#)]
65. Choi, S.H.; Stephen, B.; Park, J.-H.; Lee, J.S.; Kim, S.M.; Yang, W.; Kim, K.K. Water-Assisted Synthesis of Molybdenum Disulfide Film with Single Organic Liquid Precursor. *Sci. Rep.* **2017**, *7*, 1983. [[CrossRef](#)]
66. Kim, S.J.; Kang, M.-A.; Kim, S.H.; Lee, Y.; Song, W.; Myung, S.; Lee, S.S.; Lim, J.; An, K.-S. Large-Scale Growth and Simultaneous Doping of Molybdenum Disulfide Nanosheets. *Sci. Rep.* **2016**, *6*, 24054. [[CrossRef](#)]
67. Lee, Y.; Lee, J.; Bark, H.; Oh, I.-K.; Ryu, G.H.; Lee, Z.; Kim, H.; Cho, J.H.; Ahn, J.-H.; Lee, C. Synthesis of Wafer-Scale Uniform Molybdenum Disulfide Films with Control over the Layer Number Using a Gas Phase Sulfur Precursor. *Nanoscale* **2014**, *6*, 2821. [[CrossRef](#)]
68. Kim, H.; Park, T.; Leem, M.; Lee, H.; Ahn, W.; Lee, E.; Kim, H. Sulfidation Characteristics of Amorphous Nonstoichiometric Mo-Oxides for MoS<sub>2</sub> Synthesis. *Appl. Surf. Sci.* **2021**, *535*, 147684. [[CrossRef](#)]
69. Lin, Z.; Liu, Y.; Halim, U.; Ding, M.; Liu, Y.; Wang, Y.; Jia, C.; Chen, P.; Duan, X.; Wang, C.; et al. Solution-Processable 2D Semiconductors for High-Performance Large-Area Electronics. *Nature* **2018**, *562*, 254–258. [[CrossRef](#)]
70. Mishra, V.; Smith, S.; Ganapathi, K.; Salahuddin, S. Dependence of Intrinsic Performance of Transition Metal Dichalcogenide Transistors on Materials and Number of Layers at the 5 Nm Channel-Length Limit. In Proceedings of the 2013 IEEE International Electron Devices Meeting, Washington, DC, USA, 9–11 December 2013; IEEE: Washington, DC, USA, 2013; pp. 5.6.1–5.6.4.
71. Polyushkin, D.K.; Wachter, S.; Mennel, L.; Paur, M.; Paliy, M.; Iannaccone, G.; Fiori, G.; Neumaier, D.; Canto, B.; Mueller, T. Analogue Two-Dimensional Semiconductor Electronics. *Nat. Electron.* **2020**, *3*, 486–491. [[CrossRef](#)]

72. Esmaeili-Rad, M.R.; Salahuddin, S. High Performance Molybdenum Disulfide Amorphous Silicon Heterojunction Photodetector. *Sci. Rep.* **2013**, *3*, 6. [[CrossRef](#)]
73. Basyooni, M.A.; Zaki, S.E.; Shaban, M.; Eker, Y.R.; Yilmaz, M. Efficient MoWO<sub>3</sub>/VO<sub>2</sub>/MoS<sub>2</sub>/Si UV Schottky Photodetectors; MoS<sub>2</sub> Optimization and Monoclinic VO<sub>2</sub> Surface Modifications. *Sci. Rep.* **2020**, *10*, 15926. [[CrossRef](#)]
74. Jayachandran, D.; Oberoi, A.; Sebastian, A.; Choudhury, T.H.; Shankar, B.; Redwing, J.M.; Das, S. A Low-Power Biomimetic Collision Detector Based on an in-Memory Molybdenum Disulfide Photodetector. *Nat. Electron.* **2020**, *3*, 646–655. [[CrossRef](#)]
75. Sanjay, S.; Sahoo, K.; Bhat, N. Alcohol-Based Sulfur Treatment for Improved Performance and Yield in Local Back-Gated and Channel-Length-Scaled MoS<sub>2</sub> FETs. *IEEE Trans. Electron Devices* **2020**, *67*, 3711–3715. [[CrossRef](#)]
76. Hua, Q.; Gao, G.; Jiang, C.; Yu, J.; Sun, J.; Zhang, T.; Gao, B.; Cheng, W.; Liang, R.; Qian, H.; et al. Atomic Threshold-Switching Enabled MoS<sub>2</sub> Transistors towards Ultralow-Power Electronics. *Nat. Commun.* **2020**, *11*, 6207. [[CrossRef](#)] [[PubMed](#)]
77. Chang, K.-P.; Wang, J.-C.; Chen, C.-H.; Li, L.-J.; Lai, C.-S. Monolayer MoS<sub>2</sub> for Nonvolatile Memory Applications. In Proceedings of the 2016 13th IEEE International Conference on Solid-State and Integrated Circuit Technology (ICSICT), Hangzhou, China, 25–28 October 2016; IEEE: Hangzhou, China, 2016; pp. 489–491.
78. Yogeesh, M.; Chang, H.-Y.; Li, W.; Rahimi, S.; Rai, A.; Sanne, A.; Ghosh, R.; Banerjee, S.K.; Akinwande, D. Towards Wafer Scale Monolayer MoS<sub>2</sub> Based Flexible Low-Power RF Electronics for IoT Systems. In Proceedings of the 2016 74th Annual Device Research Conference (DRC), Newark, DE, USA, 19–22 June 2016; IEEE: Newark, DE, USA, 2016; pp. 1–2.
79. Wei, W.; Dai, Y.; Niu, C.; Huang, B. Controlling the Electronic Structures and Properties of In-Plane Transition-Metal Dichalcogenides Quantum Wells. *Sci. Rep.* **2015**, *5*, 17578. [[CrossRef](#)]
80. Terrones, H.; López-Urías, F.; Terrones, M. Novel Hetero-Layered Materials with Tunable Direct Band Gaps by Sandwiching Different Metal Disulfides and Diselenides. *Sci. Rep.* **2013**, *3*, 1549. [[CrossRef](#)]
81. Gupta, S.; Kumar, P.; Paul, T.; van Schaik, A.; Ghosh, A.; Thakur, C.S. Low Power, CMOS-MoS<sub>2</sub> Memtransistor Based Neuromorphic Hybrid Architecture for Wake-Up Systems. *Sci. Rep.* **2019**, *9*, 15604. [[CrossRef](#)]
82. Santosh, K.C.; Longo, R.C.; Addou, R.; Wallace, R.M.; Cho, K. Electronic Properties of MoS<sub>2</sub>/MoO<sub>x</sub> Interfaces: Implications in Tunnel Field Effect Transistors and Hole Contacts. *Sci. Rep.* **2016**, *6*, 33562. [[CrossRef](#)]
83. Cui, X.; Kong, Z.; Gao, E.; Huang, D.; Hao, Y.; Shen, H.; Di, C.; Xu, Z.; Zheng, J.; Zhu, D. Rolling up Transition Metal Dichalcogenide Nanoscrolls via One Drop of Ethanol. *Nat. Commun.* **2018**, *9*, 1301. [[CrossRef](#)]
84. Choi, C.; Leem, J.; Kim, M.S.; Taqieddin, A.; Cho, C.; Cho, K.W.; Lee, G.J.; Seung, H.; Bae, H.J.; Song, Y.M.; et al. Curved Neuromorphic Image Sensor Array Using a MoS<sub>2</sub>-Organic Heterostructure Inspired by the Human Visual Recognition System. *Nat. Commun.* **2020**, *11*, 5934. [[CrossRef](#)]
85. Liu, Y.; Peng, J.; Wang, S.; Xu, M.; Gao, M.; Xia, T.; Weng, J.; Xu, A.; Liu, S. Molybdenum Disulfide/Graphene Oxide Nanocomposites Show Favorable Lung Targeting and Enhanced Drug Loading/Tumor-Killing Efficacy with Improved Biocompatibility. *NPG Asia Mater.* **2018**, *10*, e458. [[CrossRef](#)]
86. Zheng, C.; Jin, X.; Li, Y.; Mei, J.; Sun, Y.; Xiao, M.; Zhang, H.; Zhang, Z.; Zhang, G.-J. Sensitive Molybdenum Disulfide Based Field Effect Transistor Sensor for Real-Time Monitoring of Hydrogen Peroxide. *Sci. Rep.* **2019**, *9*, 759. [[CrossRef](#)]
87. Ding, X.; Peng, F.; Zhou, J.; Gong, W.; Slaven, G.; Loh, K.P.; Lim, C.T.; Leong, D.T. Defect Engineered Bioactive Transition Metals Dichalcogenides Quantum Dots. *Nat. Commun.* **2019**, *10*, 41. [[CrossRef](#)]
88. Faramarzi, V.; Ahmadi, V.; Fotouhi, B.; Abasifard, M. A Potential Sensing Mechanism for DNA Nucleobases by Optical Properties of GO and MoS<sub>2</sub> Nanopores. *Sci. Rep.* **2019**, *9*, 6230. [[CrossRef](#)]
89. Singh, C.; Ali, M.A.; Kumar, V.; Ahmad, R.; Sumana, G. Functionalized MoS<sub>2</sub> Nanosheets Assembled Microfluidic Immunosensor for Highly Sensitive Detection of Food Pathogen. *Sens. Actuators B Chem.* **2018**, *259*, 1090–1098. [[CrossRef](#)]
90. Barati Farimani, A.; Heiranian, M.; Aluru, N.R. Identification of Amino Acids with Sensitive Nanoporous MoS<sub>2</sub>: Towards Machine Learning-Based Prediction. *NPJ 2D Mater. Appl.* **2018**, *2*, 14. [[CrossRef](#)]
91. Shi, T.; Hou, X.; Guo, S.; Zhang, L.; Wei, C.; Peng, T.; Hu, X. Nanohole-Boosted Electron Transport between Nanomaterials and Bacteria as a Concept for Nano–Bio Interactions. *Nat. Commun.* **2021**, *12*, 493. [[CrossRef](#)]
92. Zhang, W.; Zhang, P.; Su, Z.; Wei, G. Synthesis and Sensor Applications of MoS<sub>2</sub> -Based Nanocomposites. *Nanoscale* **2015**, *7*, 18364–18378. [[CrossRef](#)]
93. Concept for Two-Dimensional TMDs as Functional Layer for Gas Sensing Applications | VDE Conference Publication | IEEE Xplore. Available online: <https://ieeexplore.ieee.org/document/9257305> (accessed on 14 March 2021).
94. Scalable Growth of High-Quality MoS<sub>2</sub> Film by Magnetron Sputtering: Application for NO<sub>2</sub> Gas Sensing | IEEE Conference Publication | IEEE Xplore. Available online: <https://ieeexplore.ieee.org/document/9033716> (accessed on 14 March 2021).
95. Thin EOT MoS<sub>2</sub> FET for Efficient Photodetection and Gas Sensing | IEEE Conference Publication | IEEE Xplore. Available online: <https://ieeexplore.ieee.org/document/8937927> (accessed on 14 March 2021).
96. Multilayer CVD-Graphene and MoS<sub>2</sub> Ethanol Sensing and Characterization Using Kretschmann-Based SPR | IEEE Journals & Magazine | IEEE Xplore. Available online: <https://ieeexplore.ieee.org/document/9187269> (accessed on 14 March 2021).
97. Huang, Y.; Shi, Y.; Yang, H.Y.; Ai, Y. A Novel Single-Layered MoS<sub>2</sub> Nanosheet Based Microfluidic Biosensor for Ultrasensitive Detection of DNA. *Nanoscale* **2015**, *7*, 2245–2249. [[CrossRef](#)]
98. Surface Plasmon Resonance (SPR) for Sensors and Biosensors-ScienceDirect. Available online: <https://www.sciencedirect.com/science/article/pii/B9780323497787000060> (accessed on 13 March 2021).

99. Rahman, M.M.; Rahman, M.S.; Rikta, K.A.; Rana, M.M.; Anower, M.S.; Paul, A.K. Promising SPR Biosensors Applying 2D Materials with  $\alpha$ -SnSe Allotrope for Sensing Applications. In Proceedings of the 2020 IEEE Region 10 Symposium (TENSYMP); IEEE: Dhaka, Bangladesh, 2020; pp. 1197–1200.
100. Tan, Y.; He, R.; Cheng, C.; Wang, D.; Chen, Y.; Chen, F. Polarization-Dependent Optical Absorption of MoS<sub>2</sub> for Refractive Index Sensing. *Sci. Rep.* **2015**, *4*, 7523. [[CrossRef](#)]
101. Mukherjee, B.; Kaushik, N.; Tripathi, R.P.N.; Joseph, A.M.; Mohapatra, P.K.; Dhar, S.; Singh, B.P.; Kumar, G.V.P.; Simsek, E.; Lodha, S. Exciton Emission Intensity Modulation of Monolayer MoS<sub>2</sub> via Au Plasmon Coupling. *Sci. Rep.* **2017**, *7*, 41175. [[CrossRef](#)]
102. Chen, C.H.; Chang, X.; Wu, C.S. A novel shaped-controlled fabrication of nanopore and its applications in quantum electronics. *Sci. Rep.* **2019**, *9*, 18663. [[CrossRef](#)]
103. Pham, T.; Li, G.; Bekyarova, E.; Itkis, M.E.; Mulchandani, A. MoS<sub>2</sub>-Based Optoelectronic Gas Sensor with Sub-Parts-per-Billion Limit of NO<sub>2</sub> Gas Detection. *ACS Nano* **2019**, *13*, 3196–3205. [[CrossRef](#)]
104. Kinnamon, D.; Ghanta, R.; Lin, K.-C.; Muthukumar, S.; Prasad, S. Portable Biosensor for Monitoring Cortisol in Low-Volume Perspired Human Sweat. *Sci. Rep.* **2017**, *7*, 13312. [[CrossRef](#)]
105. Hwang, J.C.M. Novel Materials and Devices for Millimeter-Wave and THz Applications. In Proceedings of the 2012 IEEE MTT-S International Microwave Workshop Series on Millimeter Wave Wireless Technology and Applications, Nanjing, China, 18–20 September 2012; IEEE: Nanjing, China, 2012; p. 1.
106. Jung, Y.H.; Seo, J.-H.; Zhang, H.; Lee, J.; Cho, S.J.; Chang, T.-H.; Ma, Z. Radio-Frequency Flexible and Stretchable Electronics: The Need, Challenges and Opportunities. In Proceedings of the Micro- and Nanotechnology Sensors, Systems, and Applications IX, SPIE Defense + Security, International Society for Optics and Photonics. Anaheim, CA, USA, 18 May 2017; Volume 10194, p. 101941C. [[CrossRef](#)]
107. Dejband, E.; Karami, H.; Hosseini, M.; Torkaman, P. Switchable Abnormal THz Wave Reflector Based on Molybdenum Disulfide (MoS<sub>2</sub>). In Proceedings of the 2018 Fifth International Conference on Millimeter-Wave and Terahertz Technologies (MMWaTT), Tehran, Iran, 18–20 December 2018; IEEE: Tehran, Iran, 2018; pp. 58–61.
108. Hijazi, A.; Moutaouakil, A.E. Graphene and MoS<sub>2</sub> Structures for THz Applications. In Proceedings of the 2019 44th International Conference on Infrared, Millimeter, and Terahertz Waves (IRMMW-THz), Paris, France, 1–6 September 2019; IEEE: Paris, France, 2019; pp. 1–2.
109. Moutaouakil, A.E.; Komori, T.; Horiike, K.; Suemitsu, T.; Otsuji, T. Room Temperature Intense Terahertz Emission from a Dual Grating Gate Plasmon-Resonant Emitter Using InAlAs/InGaAs/InP Material Systems. *IEICE Trans. Electron.* **2010**, *E93.C*, 1286–1289. [[CrossRef](#)]
110. Moutaouakil, A.E. Two-Dimensional Electronic Materials for Terahertz Applications: Linking the Physical Properties with Engineering Expertise. In Proceedings of the 2018 6th International Renewable and Sustainable Energy Conference (IRSEC), Rabat, Morocco, 5–8 December 2018; pp. 1–4.
111. Moutaouakil, A.E.; Suemitsu, T.; Otsuji, T.; Coquillat, D.; Knap, W. Nonresonant Detection of Terahertz Radiation in High-Electron-Mobility Transistor Structure Using InAlAs/InGaAs/InP Material Systems at Room Temperature. *J. Nanosci. Nanotechnol.* **2012**, *12*, 6737–6740. [[CrossRef](#)]
112. Moutaouakil, A.E.; Suemitsu, T.; Otsuji, T.; Coquillat, D.; Knap, W. Room Temperature Terahertz Detection in High-Electron-Mobility Transistor Structure Using InAlAs/InGaAs/InP Material Systems. In Proceedings of the 35th International Conference on Infrared, Millimeter, and Terahertz Waves, Rome, Italy, 5–10 September 2010; IEEE: Rome, Italy, 2010; pp. 1–2.
113. Moutaouakil, A.E.; Watanabe, T.; Haibo, C.; Komori, T.; Nishimura, T.; Suemitsu, T.; Otsuji, T. Spectral Narrowing of Terahertz Emission from Super-Grating Dual-Gate Plasmon-Resonant High-Electron Mobility Transistors. *J. Phys. Conf. Ser.* **2009**, *193*, 012068. [[CrossRef](#)]
114. El Moutaouakil, A.; Suemitsu, T.; Otsuji, T.; Videlier, H.; Boubanga-Tombet, S.-A.; Coquillat, D.; Knap, W. Device Loading Effect on Nonresonant Detection of Terahertz Radiation in Dual Grating Gate Plasmon-Resonant Structure Using InGaP/InGaAs/GaAs Material Systems. *Phys. Status Solidi (C)* **2011**, *8*, 346–348. [[CrossRef](#)]
115. Cao, Y.; Gan, S.; Geng, Z.; Liu, J.; Yang, Y.; Bao, Q.; Chen, H. Optically Tuned Terahertz Modulator Based on Annealed Multilayer MoS<sub>2</sub>. *Sci. Rep.* **2016**, *6*, 22899. [[CrossRef](#)]
116. Goel, N.; Bera, J.; Kumar, R.; Sahu, S.; Kumara, M. MoS<sub>2</sub>-PVP Nanocomposites Decorated ZnO Microsheets for Efficient Hydrogen Detection. *IEEE Sens. J.* **2021**, *1*. [[CrossRef](#)]
117. Tran, P.D.; Tran, T.V.; Orio, M.; Torelli, S.; Truong, Q.D.; Nayuki, K.; Sasaki, Y.; Chiam, S.Y.; Yi, R.; Honma, I.; et al. Coordination Polymer Structure and Revisited Hydrogen Evolution Catalytic Mechanism for Amorphous Molybdenum Sulfide. *Nat. Mater.* **2016**, *15*, 640–646. [[CrossRef](#)] [[PubMed](#)]
118. Balat, M. Potential Importance of Hydrogen as a Future Solution to Environmental and Transportation Problems. *Int. J. Hydrg. Energy* **2008**, *33*, 4013–4029. [[CrossRef](#)]
119. Gao, M.-R.; Chan, M.K.Y.; Sun, Y. Edge-Terminated Molybdenum Disulfide with a 9.4-Å Interlayer Spacing for Electrochemical Hydrogen Production. *Nat. Commun.* **2015**, *6*, 7493. [[CrossRef](#)]
120. Saha, D.; Kruse, P. Editors' Choice—Review—Conductive Forms of MoS<sub>2</sub> and Their Applications in Energy Storage and Conversion. *J. Electrochem. Soc.* **2020**, *167*, 126517. [[CrossRef](#)]
121. Wang, Z.; Mi, B. Environmental Applications of 2D Molybdenum Disulfide (MoS<sub>2</sub>) Nanosheets. *Environ. Sci. Technol.* **2017**, *51*, 8229–8244. [[CrossRef](#)]

122. Gao, X.; Wang, X.; Ouyang, X.; Wen, C. Flexible Superhydrophobic and Superoleophilic MoS<sub>2</sub> Sponge for Highly Efficient Oil-Water Separation. *Sci. Rep.* **2016**, *6*, 27207. [\[CrossRef\]](#)
123. Dey, M.; Dey, M.; Alam, S.; Das, N.K.; Matin, M.A.; Amin, N. Study of Molybdenum Sulphide as a Novel Buffer Layer for CZTS Solar Cells. In Proceedings of the 2016 3rd International Conference on Electrical Engineering and Information Communication Technology (ICEEICT), Dhaka, Bangladesh, 22–24 September 2016; IEEE: Dhaka, Bangladesh, 2016; pp. 1–4.
124. Iqbal, M.Z.; Nabi, J.; Siddique, S.; Awan, H.T.A.; Haider, S.S.; Sulman, M. Role of Graphene and Transition Metal Dichalcogenides as Hole Transport Layer and Counter Electrode in Solar Cells. *Int. J. Energy Res.* **2020**, *44*, 1464–1487. [\[CrossRef\]](#)
125. Capasso, A.; Del Rio Castillo, A.E.; Najafi, L.; Pellegrini, V.; Bonaccorso, F.; Matteocci, F.; Cina, L.; Di Carlo, A. Spray Deposition of Exfoliated MoS<sub>2</sub> Flakes as Hole Transport Layer in Perovskite-Based Photovoltaics. In Proceedings of the 2015 IEEE 15th International Conference on Nanotechnology (IEEE-NANO), Rome, Italy, 27–30 July 2015; IEEE: Rome, Italy, 2015; pp. 1138–1141.
126. Xu, H.; Xin, L.; Liu, L.; Pang, D.; Jiao, Y.; Cong, R.; Yu, W. Large Area MoS<sub>2</sub>/Si Heterojunction-Based Solar Cell through Sol-Gel Method. *Mater. Lett.* **2019**, *238*, 13–16. [\[CrossRef\]](#)
127. Liang, M.; Ali, A.; Belaidi, A.; Hossain, M.I.; Ronan, O.; Downing, C.; Tabet, N.; Sanvito, S.; El-Mellouhi, F.; Nicolosi, V. Improving Stability of Organometallic-Halide Perovskite Solar Cells Using Exfoliation Two-Dimensional Molybdenum Chalcogenides. *NPJ 2D Mater. Appl.* **2020**, *4*, 40. [\[CrossRef\]](#)
128. Huang, Y.; Wang, Y.; Zhang, X.; Lai, F.; Sun, Y.; Li, Q.; Wang, H. N-Doped Carbon@nanoplate-Assembled MoS<sub>2</sub> Hierarchical Microspheres as Anode Material for Lithium-Ion Batteries. *Mater. Lett.* **2019**, *243*, 84–87. [\[CrossRef\]](#)
129. Bao, W.; Cai, X.; Kim, D.; Sridhara, K.; Fuhrer, M.S. High Mobility Ambipolar MoS<sub>2</sub> Field-Effect Transistors: Substrate and Dielectric Effects. *Appl. Phys. Lett.* **2013**, *102*, 042104. [\[CrossRef\]](#)
130. Kramer, A.; Van de Put, M.L.; Hinkle, C.L.; Vandenberghe, W.G. Tellurium as a Successor of Silicon for Extremely Scaled Nanowires: A First-Principles Study. *NPJ 2D Mater. Appl.* **2020**, *4*, 10. [\[CrossRef\]](#)
131. Manzeli, S.; Ovchinnikov, D.; Pasquier, D.; Yazyev, O.V.; Kis, A. 2D Transition Metal Dichalcogenides. *Nat. Rev. Mater.* **2017**, *2*, 17033. [\[CrossRef\]](#)
132. Cao, W.; Kang, J.; Sarkar, D.; Liu, W.; Banerjee, K. 2D Semiconductor FETs—Projections and Design for Sub-10 Nm VLSI. *IEEE Trans. Electron Devices* **2015**, *62*, 3459–3469. [\[CrossRef\]](#)
133. Wang, H.; Li, C.; Fang, P.; Zhang, Z.; Zhang, J.Z. Synthesis, Properties, and Optoelectronic Applications of Two-Dimensional MoS<sub>2</sub> and MoS<sub>2</sub>-Based Heterostructures. *Chem. Soc. Rev.* **2018**, *47*, 6101–6127. [\[CrossRef\]](#)
134. Stroud, A.; Derosa, P.A.; Leuty, G.; Muratore, C.; Berry, R.; Muratory, C. Effects of Impurities and Lattice Imperfections on the Conductive Properties of MoS<sub>2</sub>. In Proceedings of the 2015 IEEE 15th International Conference on Nanotechnology (IEEE-NANO), Rome, Italy, 27–30 July 2015; IEEE: Rome, Italy, 2015; pp. 613–616.
135. Yu, S.; Wu, X.; Wang, Y.; Guo, X.; Tong, L. 2D Materials for Optical Modulation: Challenges and Opportunities. *Adv. Mater.* **2017**, *29*, 1606128. [\[CrossRef\]](#)
136. Chen, X.; Shinde, S.M.; Dhakal, K.P.; Lee, S.W.; Kim, H.; Lee, Z.; Ahn, J.-H. Degradation Behaviors and Mechanisms of MoS<sub>2</sub> Crystals Relevant to Bioabsorbable Electronics. *NPG Asia Mater.* **2018**, *10*, 810–820. [\[CrossRef\]](#)
137. Shree, S.; Paradisanos, I.; Marie, X.; Robert, C.; Urbaszek, B. Guide to Optical Spectroscopy of Layered Semiconductors. *Nat. Rev. Phys.* **2021**, *3*, 39–54. [\[CrossRef\]](#)
138. Peng, Z.; Chen, X.; Fan, Y.; Srolovitz, D.J.; Lei, D. Strain Engineering of 2D Semiconductors and Graphene: From Strain Fields to Band-Structure Tuning and Photonic Applications. *Light. Sci. Appl.* **2020**, *9*, 190. [\[CrossRef\]](#)
139. Fan, X.; Zheng, W.T.; Kuo, J.-L.; Singh, D.J. Structural Stability of Single-Layer MoS<sub>2</sub> under Large Strain. *J. Phys. Condens. Matter* **2015**, *27*, 105401. [\[CrossRef\]](#)
140. Kumar, P.; Horwath, J.P.; Foucher, A.C.; Price, C.C.; Acero, N.; Shenoy, V.B.; Stach, E.A.; Jariwala, D. Direct Visualization of Out-of-Equilibrium Structural Transformations in Atomically Thin Chalcogenides. *NPJ 2D Mater. Appl.* **2020**, *4*, 16. [\[CrossRef\]](#)
141. Kaur, J.; Singh, M.; Dell’Aversana, C.; Benedetti, R.; Giardina, P.; Rossi, M.; Valadan, M.; Vergara, A.; Cutarelli, A.; Montone, A.M.I.; et al. Biological Interactions of Biocompatible and Water-Dispersed MoS<sub>2</sub> Nanosheets with Bacteria and Human Cells. *Sci. Rep.* **2018**, *8*, 16386. [\[CrossRef\]](#)
142. Wu, B.; Chen, L.; Wu, X.; Hou, H.; Wang, Z.; Liu, S. Differential Influence of Molybdenum Disulfide at the Nanometer and Micron Scales in the Intestinal Metabolome and Microbiome of Mice. *Environ. Sci. Nano* **2019**, *6*, 1594–1606. [\[CrossRef\]](#)